CHAPTER 5

EXPERIMENTAL PROCEDURES AND RESULTS

The experimental procedures conducted during the study comprised the following:

- Analyses of existing hydrogeological data obtained from literature. Data on soil fractions, soil-water retention characteristics and saturated and unsaturated hydraulic conductivities were obtained for soils ranging from coarse sand to clay. Empirical relationships, as described in Chapter 4, were applied to these data and the accuracy and validity of these relationships were assessed.

- Laboratory tests were conducted on three soil types to determine the geotechnical and hydrogeological properties. The geotechnical data were used to predict hydrogeological properties and these were compared to measured hydrogeological properties.

- Field tests were conducted on three soil types to determine the *in situ* hydrogeological properties of these soils. The *in situ* properties were compared to small-scale laboratory results. In addition, the effect of preferential flow, in particular macropore channelling, was assessed for the three soil types.

Because of the number of factors that could influence the hydrogeological properties (including parent rock type, climate, vegetation and time), the research focussed on the characterisation of hydrogeological properties of residual granite. Two experiments were conducted on residual andesite.

5.1 Experimental laboratory and literature studies

Empirical equations relating physical soil properties with hydrogeological properties within the vadose zone were analysed in order to assess the accuracy and reliability of predicted hydrogeological properties. These analyses are mainly based on geohydrological data obtained from literature. The following relationships were investigated:

- Relationship between saturated hydraulic conductivity and physical soil properties (fractions sand, silt and clay, particle-size distribution curves and soil water retention characteristics)

- Analyses of functions describing the soil-water characteristic curve

- Relationship between unsaturated hydraulic conductivity and physical soil properties (fractions sand, silt and clay and particle-size distribution curves)

- Relationship between unsaturated hydraulic conductivity and the soil-water characteristic curve

Various empirical equations were developed (as discussed in Chapter 4) to predict the saturated hydraulic conductivity from sand, silt and clay fractions (soil texture data). In order to assess the reliability of these relationships, the equations were applied to a wide range of literature-based soil data. Basic soil data were obtained from published data sources, such as these published by the Desert Research Institute (1983). A total of 26 data points, representing soils ranging from clay to sand, were applied to the empirical relationships as established in Chapter 4. Saturated hydraulic conductivities were predicted from soil fractions, particle-size distribution curves and soil-water retention data. The predicted values were compared to measured saturated hydraulic conductivity data.

Several mathematical functions describing the soil-water characteristic curve were discussed in Chapter 4. Reliable indirect estimations of unsaturated hydraulic conductivity, based on soil-water retention curves, are only possible on condition that these mathematical functions accurately describe the soil-water characteristic curve. Since the soil-water characteristic curve may be either exponential or sigmoidal in shape (depending on the type of soil), the development of a single function that is valid for all soil-water characteristic curve shapes is complicated.

Several popular functions used to describe the soil-water characteristic curve were tested for five different soil types. These functions were applied to soil-water retention data obtained from literature. A large amount of unsaturated flow data was collected, analysed and published by the Desert Research Institute (1983).

It has already been shown that the soil-water characteristic curves for five soil types can be accurately described by the Van Genucten and Fredlund and Xing functions. These data-sets were further analysed to determine the unsaturated hydraulic conductivity in terms of the Van Genucten and Fredlund *et al.* models. The calculated values were compared to experimentally determined unsaturated hydraulic conductivity values.

5.2 Field experiments

Five extensive field experiments were conducted during the period October 1995 to June 1997. The field experiments were conducted for the following reasons:

- To study the effect of preferential flow and the variability of hydrogeological properties in field soils.
- To study the reliability of existing empirical and other models in estimating the geohydrological properties of field soils

It was impossible to cover all types of residual soils with the field experiments. It was decided to focus on a specific soil and to establish a workable experimental methodology that could be applied in future research. After considering the different types of residual soils, it was decided to focus on residual granite since it covers large parts of South Africa and little is known about its hydrogeological properties. Consequently, Experiments 3, 4 and 5 were conducted on residual granite.

The site of Experiments 1 and 2 is predominantly underlain by andesite of the Hekpoort Formation, Pretoria Group, Transvaal Sequence. Diabase dyke intrusions are also present. Andesite mainly comprises plagioclase with smaller amounts of clino-pyroxene, hornblende and mica. The Weinert N-value for Pretoria is 2.4 (Weinert, 1980). This value suggests predominant chemical weathering and the development of clay minerals such as kaolinite in silica over-saturated rocks and montmorillonite in silica under-saturated rocks.

Experiments 3 and 4 were conducted at Midrand. Experiment 3 was conducted during March 1996, close to the N1 highway near the Samrand onramp. The area was at the time being developed into the Samrand industrial zone. Because of the presence of ferruginised soil with low permeability, a shallow bedrock

and seepage into the testpit, the geohydrological properties could not be derived and the experiment was abandoned.

Experiment 4 was conducted in deeper weathered, less ferruginised soil during the months of April to August 1996. It was conducted close to the New Road and N1 highway intersection, which was under construction at the time.

The sites for Experiments 3 and 4 are underlain by the Halfway House Granite Suite, which mainly comprises granitic gneiss of the Basement Complex. The formation of residual soil has largely been affected by palaeo-climate. Areas above 1 600 m a.m.s.l. are largely remnants of the African erosion cycle, caused by a vertical upliftment of at least 1 000 m that occurred in the early Cretaceous period, which continued for more than 30 million years (Brink, 1979). The very high degree of weathering results in deep residual soil, formation of laterite and even bauxite and intense leaching. The Weinert N-value of 2.4 (Weinert, 1980) suggests predominant chemical weathering, as in the case of Experiments 1 and 2.

The geology at Experiment 4 is representative of the African erosion cycle. Deep residual and completely weathered granite occurs to a depth of more than 10 m. The geology is affected by human activities since the site is in a developed area. The site is also characterised by leached soil layers due to weathering over a long time. Granite corestones are abundant, e.g. the huge granite core stones in the nearby Boulders Shopping Centre. Soil properties have been expected to vary significantly both vertically and horizontally in a soil profile and a very complex flow of water through the residual soil was expected.

The site at experiment 5 is underlain by the Nelspruit Granite Suite. It comprises mostly medium to coarse-grained porphyritic biotite granite of the Basement Complex and is of Swazian age (4 000 to 2 900 Ma). Fine to medium-grained diabase intrusions of Vaalium age (2 100 to 2 700 Ma), occur frequently. The Weinert N-value (1980) is 2.0, suggesting predominant chemical weathering, as is the case in the other experiments.

5.2.1 The effect of preferential pathways and soil variability

Field soils generally comprise distinct layers, developed by the process of pedogenesis. These layers may cause fingering and funnelled flow while macropores, caused by *inter alia* plant-root penetration and desiccation, could cause macropore-channelling

According to the concept of the Representative Elementary Volume (Chapter 4), the effect of preferential flow (if any) should be detected if a sufficiently large representative volume is tested. According to Lauren *et al.* (1988), the REV for soils with macropores is 0.125 m^3 and according to Inoue *et al.* (1988), the REV for soils with cracks is 125 m^3. If no preferential flow is detected in the course of testing these samples, preferential flow paths may still occur in the field soil, but its effect in transporting water and contaminants to the groundwater regime is probably negligible. The exception is highly toxic substances such as pesticides, which could be hazardous even in minute quantities.

Large soil volumes were tested by conducting large-scale *in situ* tests and it was assumed that results will include the effect of preferential flow. In addition, block samples, which do *not* contain any cracks, fissures or biopores, have been carefully selected and the result of these represent matrix flow. In comparing field test results with laboratory results, it could be concluded that higher flow velocities in field soils would suggest the presence of significant preferential flow.

The small laboratory samples used in permeability tests may not be representative of field matrix soils due to the high variability of dry density, soil composition and other properties, resulting in large variations in laboratory-determined hydraulic conductivity values.

5.2.2 Calibration of the neutron probe

A CPN 503 DR hydroprobe® was used to measure *in situ* soil moisture content during the field experiments. The change in moisture content during both infiltration and drainage were measured which assisted in determining geohydrological parameters, such as saturated and unsaturated hydraulic conductivity.

The neutron probe works on the principle of neutron-matter interaction. High-energy neutrons emitted from a radioactive source are thermalised (slowed down) by collisions with atomic nuclei. Hydrogen causes a greater thermalising effect than many other elements found in the soil. The capture of these thermalised neutrons forms the basis for detecting the quantity of water in the soil.

The neutron probe has to be calibrated for the different soil types. The neutron probe calibration method has to take into account both water content and *in situ* density, since both affect neutron probe readings. Actual water contents were obtained by the gravimetric method. Five undisturbed samples were obtained from a site that was covered by a PVC sheet and left for one month to allow drainage to take place. The volume and weight of the samples were determined after which they were oven-dried at 110°C for 48 hours. The dry weights were then determined. Volumetric water contents, θ, were obtained and plotted against the neutron probe readings at the same depth. Linear regression was applied, using the least square method to determine the relationship between neutron probe readings and actual volumetric water content. This method was applied to every soil layer where large differences in soil density were suspected.

5.2.3 Large-Diameter Double-Ring Infiltrometer tests

In order to investigate the effect of preferential flow, Large-Diameter Double-Ring Infiltrometer (LDDRI) tests were conducted at the experimental sites. The test was conducted according to the same principle as traditional double-ring infiltrometer tests, with the exception that the diameters of the rings were three times the size of standard double-ring infiltrometers. The purpose of the larger diameter rings was to test a larger, and therefore, more representative, volume of soil. In addition, a neutron probe was used to determine the depth to wetting front, instead of excavating a hole and visually determining the depth of the wetting front. The advantage was that a number of tests could be conducted at various hydraulic heads and that the reliability of the saturated hydraulic conductivity could be quantified.

LDDRI tests were conducted according to Daniel's method (Daniel, 1989). Two corrugated iron rings, 1.45 and 3.00 m in diameter respectively, were installed concentrically, and embedded approximately 10cm in the soil. The rings were then sealed with a soil/bentonite mixture. A neutron probe access hole was made in the centre of the rings. The hole was equipped with a 2.2m long PVC neutron probe access tube. The PVC tube was sealed by a soil/bentonite mixture. The set-up of the LDDRI test is shown in **Figure 5.1**.

After saturation had been reached, water was kept at a constant head and the infiltration rate of the inner ring was determined. Infiltration rates were determined with water levels kept constant at various heights ranging from 0.05m to 0.25m.

The rate of infiltration, I, can be calculated by means of the following equation:

$$I = \frac{Q}{At} = \frac{q}{A} \qquad [5\text{-}6]$$

The saturated hydraulic conductivity value can be calculated from the following equation:

$$K_s = \frac{I}{i} = \frac{I}{1 + \frac{h}{L_f} + \psi_f} \qquad [5\text{-}7]$$

Figure 5.1: Set-up of the Large-Diameter Double-Ring Infiltration tests

Continuous infiltration for one month at Experiment 2, one week at Experiment 4 and two days at Experiment 5 prior to LDDRI tests, resulted in almost saturated conditions, providing therefore that the effect of soil suction at the wetting front was negligible.

The length of the flow path could be obtained from neutron probe readings. After infiltration of the inner-ring had been measured, neutron probe readings were taken at 5cm intervals. The wetting front could be identified by a distinct decrease in neutron probe counts.

Various assumptions were made with regard to the LDDRI tests (Daniel, 1989):

- The soil is homogeneous and uniformly wetted
- The infiltration rate is high enough to ensure accurate measurements
- Evaporation is negligible
- Seepage beneath the inner ring is one-dimensional
- The swelling process in the soil has been completed
- The effect of boundaries is negligible.

5.2.4 Internal drainage tests

After the LDDRI tests had been completed, the water in the inner and outer rings was allowed to drain. Frequent neutron probe measurements were made to determine the change of water content with time. Potential water losses due to evaporation were limited by covering the site with a canvas tent and by performing tests on deeper soil layers.

The θ-method involves application of the following empirical expressions to determine the relative hydraulic conductivity as a function of water content, θ (Fuller & Moolman, 1989):

$$\theta_s - \theta = \frac{\ln(t)}{\beta} + \frac{1}{\beta} \cdot \ln\left(\frac{\beta K_s}{\alpha z}\right) \quad [5\text{-}8]$$

and

$$K_r(\theta) = \exp[\beta(\theta - \theta_s)] \quad [5\text{-}9]$$

where θ is the volumetric water content, θ_s is water content at saturation, t is time in seconds, K_s is the saturated hydraulic conductivity, K_r is the relative hydraulic conductivity as a function of water content, z is the depth of the soil layer and α and β are constants to be determined experimentally.

Using the data at various depths in Experiment 2 and 4, a linear regression curve was fitted to a plot of (θ_s-θ) vs. ln(t) using the least squares method. The values of β and K_s could then be determined by means of Equation 5-8 and the value of K_r by means of Equation 5-9.

5.3 Experimental procedure

5.3.1 Experiment 1: UP Experimental Farm

The set-up for Experiment 1 is shown in **Figure 5.2**. Three trenches were excavated in a Z-shape as shown in the figure. The southern and western trenches were 4.2 m and 3.9 m deep respectively. Excavation went smoothly and there was no refusal. Another hole, the infiltration source hole, was hand-dug 1.0m away from the southern and western trenches. The hole was 1.00m × 0.75m in area and 1.7m deep.

Six neutron probe access holes with diameters of 50 mm were made around the infiltration source hole and in the side of the western trench as shown in **Figure 5.2**. Access holes no's. 4 and 5 were drilled in the side of the western trench at angles of 45° and 50° respectively. The ends of these access holes were directly beneath the source hole. The holes were drilled with a *Little Beaver* hydraulic 50 mm diameter auger machine. The access holes were equipped with 2.2m PVC access tubes.

The whole experimental set-up was covered by a 5m × 5m canvas tent. The tent prevented evaporation and infiltration from external sources. Background neutron probe readings were made prior to the experiment. The background readings were extended to two weeks because of heavy rain during the first week.

The source hole was filled with water and kept at a constant level of 1 m by means of a ball-valve. The water level was then allowed to drop to 40 cm. Neutron probe readings and visual inspection (including the observation of water flow through the wall of the trench) was performed three times a week.

The experiment was abandoned after the trench walls collapsed. No data with regard to drainage were obtained and it was decided that a second experiment, close to the original site, had to be conducted.

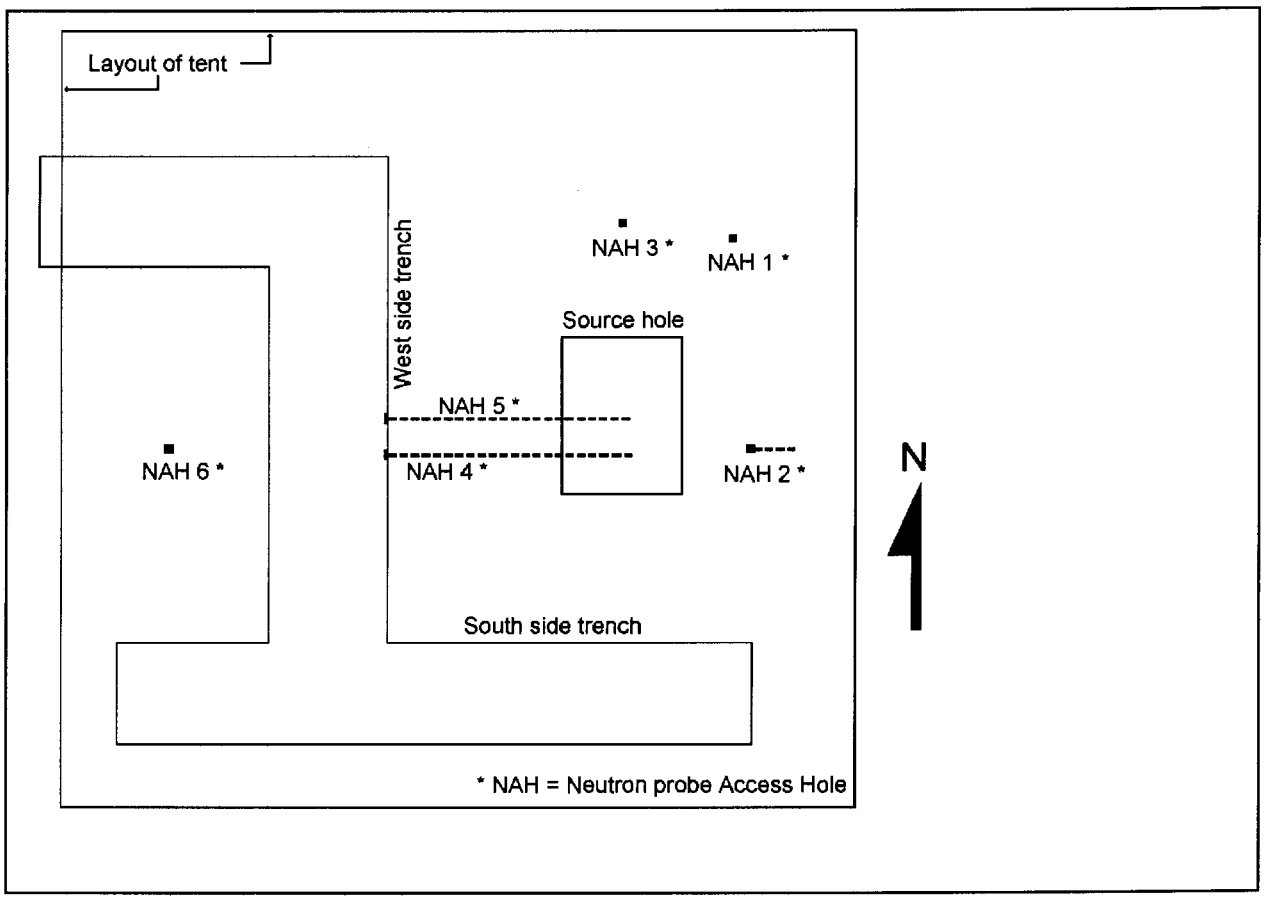

Figure 5.2: Layout of experiment 1

5.3.2 Experiment 2: UP Experimental Farm

For Experiment 2 it was decided that trenches should be excavated after infiltration had taken place. A major disadvantage of this approach was that the travel-time of water along preferential pathways could not be obtained.

A hole, 3.2 m in diameter and 0.6 m deep, was hand-dug to remove the transported material. Equipment for the LDDRI tests was installed and neutron probe background readings were taken. Water was let into both rings and kept at a constant level of 10 cm. Neutron probe readings were taken daily for one week. Constant neutron probe readings implied that saturation had been reached. The water was then allowed to drain for a few hours, after which two LDDRI tests were conducted. Hydraulic conductivity values were determined at hydraulic heads of 0.06 m and 0.25 m respectively. The soil was then allowed to drain and internal drainage tests were conducted by taking neutron probe readings once daily for one month.

After significant drainage, a trench was excavated along one side of the hole to describe the soil profile and obtain samples for geotechnical testing and to calibrate the neutron probe. Water was again let into the inner-ring and the soil profile was observed for preferential flow, but none was detected.

5.3.3 Experiment 3: Shell Ultra City, Midrand

The geology at Experiment 3 comprised of shallow ferruginised soil layer underlain by residual granite and shallow bedrock at about 3m in depth. A hole, 3.2 × 3.2 × 1.5 metres deep was excavated in order to conduct LDDRI tests on residual granite, occurring below the ferruginised layer, because that was more representative of the regional geology. The LDDRI equipment was installed in the soil and the rings

filled with water to a level of 0.20m. After about two weeks, the water level in the rings rose to 0.40 metres because of seepage. The test was abandoned and a new site, with no ferruginised layers and a deeper weathering profile, was identified.

5.3.4 Experiment 4: New Road Interchange, Midrand

Approximately 0.50 metres of transported material was removed and LDDRI equipment was installed in residual soil. After neutron probe background readings had been taken, water was let into the rings and kept at a constant level of about 10cm. Neutron probe readings were taken three to four times a day for one week, until saturation was reached. The water was then allowed to drain for two hours and five LDDRI tests were conducted. The hydraulic head was kept constant at levels varying from 0.09 m to 0.23 m. The water was then allowed to drain and an internal drainage test was conducted by means of neutron readings once a day.

After the internal drainage test, a tracer was discharged into the soil. The tracer consisted of 0.6l commercial food colouring that was diluted with about 2l water that was allowed to drain into the soil for 24 hours. A trench 3.6m deep was then excavated at the place of infiltration and the flow path of the tracer was observed visually and described. A soil profile description was recorded and samples were taken for geotechnical and water retention tests.

5.3.5 Experiment 5: Injaka dam construction site

The top 2 to 3 m of soil was removed during site preparation for grouting tests, conducted close to Experiment 5. The site was levelled and LDDRI equipment was installed in the residual soil. Heavy rains were experienced that lasted for two days but with no significant effect on the test. After neutron probe background readings had been taken, water was let into the rings and kept at a constant level of about 10 cm. Neutron probe readings were taken every hour for about eight hours after which it was continued four times a day. Saturation was reached after 48 hours. The water was then allowed to drain for two hours and six LDDRI tests were conducted. The hydraulic head was kept constant at levels varying from 0.04 m to 0.18 m. The water was then allowed to drain. A test to determine the saturated hydraulic conductivity was conducted, involving the neutron probe readings for the first two hours of drainage and applying the continuity equation.

A trench was excavated close to the inner-ring after which a soil profile description was recorded and samples taken for geotechnical and water retention tests. The inner-ring was again filled with water and the soil profile was observed for preferential flow. However, none was detected.

5.4 Geotechnical tests and results

For the purpose of this study, only the basic geotechnical data, that are generally available at various institutions in South Africa (Milford, 1994) and can be used to estimate important hydrogeological properties over large parts in South Africa, were obtained. These geotechnical tests include:

- Soil profile descriptions
- Laboratory tests to determine the index properties of soil
- Laboratory tests to determine the dry density, water content and specific gravity of the soil
- Permeability tests

In addition to the geotechnical tests, the water retention characteristics of the soil were obtained. These data can be used to establish the hydrogeological properties of unsaturated soil. The determination of soil-water characteristic curves is not a typical geotechnical test, but agricultural water retention data is readily available.

5.4.1 Soil profile descriptions

Soil profile descriptions were recorded at all experimental sites and described according to the guidelines of Jennings *et al.* (1973). In addition, four exploratory large-diameter auger holes were made at the sites of Experiments 1 and 2. Earth cuttings made during the construction of the road onramp at Midrand and the Injaka dam were also studied.

The soil profiles at Experiments 1 and 2 generally comprise a 0.5 m thick, dark-brown, micro-shattered hillwash, overlying a brownish dark-red, firm, silty clay with sand up to about 2.5 m thick. This layer is underlain by reddish yellow, fissured, clayey silt with an increasing sand content to the end of the auger holes at 7 m. Kaolonite clods are discernible at a depth of 1.1m. No water was encountered during the auger drilling, implying that the groundwater surface is deeper than seven metres. Desiccation cracks appeared on trench walls. Plant roots were observed in the soil profile up to a depth of 4 m. The dark-red clayey silt is the result of pedogenesis that destroyed all relict rock structures except for isolated disintegrated quartz veins. The yellow fissured clayey silt was interpreted as completely weathered andesite and the fissures were interpreted as relict bedding or foliation planes. The transition between the red clayey silt and the yellow fissured clayey silt is uneven and gradual. Occasional red 'fingers' intrude into the yellow fissured clayey silt. The depth of this transitional zone varied from 2.0 m to 3.0 m. The finger-like structures were probably caused by preferential weathering along rock joints.

The soil profile at Experiment 3 comprises of about 0.5m, loose to medium dense, clayey fine sand hillwash, underlain by about 2 m of ferruginised residual granite. Shallow granite bedrock was encountered at about 3 m and shallow groundwater at about 2.5 m.

The soil profile at Experiment 4 comprises about 2.0m deep, brownish dark red, very dense to medium dense, clayey, fine sand with gravel; residual granite. This layer is underlain by a 1.0m deep, brownish red mottled yellow and orange, loose, leached, micaceous, medium to coarse sand. The leached layer represents intense weathering, leaching and lessivage over a long period of time, typical of soils developed on the African erosion surface. The leached layer is underlain by a brownish red, orange and yellow, medium dense, micaceous, completely weathered granite. The construction of a new highway onramp at the New Road/N1 intersection revealed a 6m deep and 30m long section through residual and completely weathered granite. The section comprises a dark red oxidised, residual granite and completely weathered granite underlain by greyish white, kaolinitic, completely weathered granite. A clear transition between the greyish white and dark red completely weathered granite and dark red root-like structures extended within the greyish white completely weathered granite. This was probably caused by preferential weathering along discontinuities within granite rock. Large granite corestones were excavated during construction and quartz veins were also visible.

The geology at Experiment 5 comprises more than 10m of deeply weathered, residual and completely weathered granite. A relatively low quartz content was noticeable. The prevailing humid conditions resulted in predominant chemical weathering and the formation of clay minerals in a deep soil profile. The soil profile at Experiment 5 comprised a 2 to 3 metres thick dark red silty sand with clay overlying a white and yellowish light red gravelly sand layer. The top layer was removed during clearing and levelling of the site for preparation of grouting tests. The soil profile was therefore recorded about 4 metres below the natural ground surface.

No distinct soil layers were noticed in the recorded soil profile. Weathering tends to be controlled by relict rock structures and preferential weathering zones and the soil profile was therefore described as different zones rather than the traditional soil layers. The soil profile generally comprises gravelly,

coarse, medium and fine sand with silt. The soil zones differ slightly in colour and silt content, with the exception of a dark red clayey sand pocket and a highly weathered quartz-pegmatite zone. Relict rock fractures could easily be identified from discoloration on the fracture surfaces. Plant-roots frequently occur along these fractures.

A dark red, clayey, fine and medium sand with clay, soil pocket (20 cm × 30 cm) was observed at a depth of about 0.90 metres. This soil pocket differed markedly from the surrounding soil in colour and soil type, but was similar to the top dark red soil layer (that had been removed). A complicated plant-root structure was observed within this soil pocket. It is postulated that this soil pocket has formed due to preferential weathering along a non-resistant weathering zone within the parent rock. The soil weathered to a clayey sand and plant roots took advantage of the higher water content in the clayey soil which resulted in further weathering.

The soil profiles are presented in **Appendix A.**

5.4.2 Geotechnical laboratory tests

A total of 13 disturbed and 37 block samples were obtained from the five experimental areas. 13 indicator tests, 13 basic geotechnical tests consisting of bulk density, moisture content and specific gravity tests and 13 falling-head permeability tests were conducted by the Department of Water Affairs and Forestry's soil materials laboratory. The results are summarised in **Table 5.1.**

Table 5.1: Average values for geotechnical properties of soil samples

	Experiments 1 and 2	**Experiments 3 and 4**	**Experiment 5**
Index properties (%)	**n = 4**	**n = 5**	**n = 4**
Gravel	0.0	22.0	1.00
Sand	26.5	50.8	59.0
Silt	39.5	17.0	28.1
Clay	34.1	7.4	11.8
Liquid limit	44.7	30.2	38.8
Plasticity index	18.5	10.7	13.48
Shrinkage limit	8.9	5.3	5.5
Basic geotechnical properties	**n = 5**	**n=3**	**n=5**
Dry density	1 406 kg/m^3	1668 kg/m^3	1445 kg/m^3
Specific gravity of the solids	2.61	2.64	2.65
Mass water content	24.8%	13.6%	19.12%
Volumetric water content	36.5%	25.8%	27.6%
Porosity	46.2%	36.8%	45.5%
Void ratio	0.86	0.58	0.84
Degree of saturation	79.7%	70.4%	60.73%
Hydraulic conductivity (m/s)	**n=4**	**n=4**	**n=5**
Average value	2.17×10^{-7}	7.64×10^{-8}	1.36×10^{-6}
Median value	7.10×10^{-9}	1.75×10^{-8}	9.80×10^{-7}

n = number of samples

The soil samples in Experiments 1 and 2 comprised well-graded, fine, silty clays. Low liquid and plasticity limits resulted in low activity values, except for samples I-103 and I-107 that were characterised by high liquid and plasticity limits and a high activity value. The samples were classified according to the USCS as silt with sand (ML) to clay with low plasticity with sand (CL), except for samples I-103 and I-107 that were classified as clay with high plasticity with sand (CH) and silt (MH) respectively. The

higher permeability values of sample I-101 can be attributed to by-pass flow of water along the sides of the soil samples during testing.

Soil samples at Experiments 3 and 4, typically comprised well-graded, gravelly clayey sands, some with significant silt contents. All the samples were characterised by low liquid and plasticity limit values and low activity values resulting from the low clay contents. The samples were classified as clayey sands (SC) according to the USCS.

Soil samples at Experiment 5 typically comprised well-graded sands with little silt and clay, the exception being sample I-501, which comprised clayey, fine sand. Sample I-501 was obtained from the dark red clayey sand pocket, and was characterised by a high plasticity index and subsequently a high activity, unlike the other samples, which were characterised by low plasticity indices and low activities. The samples were classified as clayey sands (SC) according to the USCS, with the exception of sample I-501, which was classified as a inorganic clay with high plasticity (CH). It is worthwhile to observe that the soil was classified as a clayey sand, although the sand and silt fraction together amount to only 8 to 10 per cent of the sample weight. This can be explained by the relatively high fine sand fraction (27 to 31 per cent of the sample weight) that is included with the fine fraction.

The geotechnical results are presented in **Appendix B**.

The natural variability of soil properties in field soils was investigated, using statistical analysis of the geotechnical data and calculating the coefficient of variability. The coefficient of variability was used instead of the more traditional standard deviation in order to compare the variability of different soil properties with each other. The results are presented in **Table 5.2**.

Table 5.2: Coefficient of Variability of geotechnical properties

	Coefficient of Variability (%)		
	Experiments 1 and 2	**Experiments 3 and 4**	**Experiment 5**
Index properties	**n = 4**	**n=5**	**n=4**
Gravel	N.A.	12.03	141.42
Sand	22.80	16.26	22.66
Silt	8.23	16.11	6.05
Clay	25.68	68.64	115.10
Liquid limit	19.60	5.46	24.72
Plasticity index	36.24	25.45	67.00
Shrinkage limit	34.27	27.06	79.45
Basic geotechnical properties	**n = 5**	**n=3**	**n=5**
Dry density	4.74	3.33	2.84
Specific gravity of the solids	5.49	0.44	0.63
Mass water content	12.91	2.55	10.67
Volumetric water content	10.24	5.47	10.79
Porosity	6.82	6.10	3.98
Void ratio	11.99	9.44	7.39
Degree of saturation	16.22	11.42	12.29
Hydraulic conductivity	**n=4**	**n=4**	**n=5**
Hydraulic conductivity	194.84	170.00	77.69

n = number of samples

In general, the variability of basic geotechnical properties was low, while that of the index properties was low to medium. The higher variability in Atterberg limits could be caused by the subjective way in which the plasticity and shrinkage limits are determined. The liquid limit, determined in a more objective way, exhibits lower variability. The anomalous variability of the gravel proportion in Experiment 5 and the

clay proportion in Experiments 3 and 4 can be ascribed to very low gravel and clay contents respectively. Although these are highly variable compared to fractions of other soil samples, they are much less variable compared to the compositions of whole samples. The higher variability of index tests in Experiment 5, especially the clay fraction, is the result of the inclusion of sample I-301, exhibiting discrepant soil properties but representing a very small part of the soil profile. The very high variability of hydraulic conductivity values is caused by the combined effect of variability in soil composition, bulk density and other factors influencing hydraulic conductivity. The hydraulic conductivity as determined from laboratory tests is not representative of the field soil. Large-size soil samples or *in situ* tests provided more representative values.

5.4.3 Results of the water retention tests

In addition to geotechnical tests, 11 undisturbed samples were tested by *Central Agricultural Laboratories* in Pelindaba to obtain water retention characteristics. These values could be used to obtain soil-water characteristic curves. The samples were subjected to suction values of 10, 20, 50 and 100 kPa respectively and the volumetric water content was determined at each suction value. The results of these tests are shown in **Table 5.3** and the variability of water retention characteristics is indicated in **Table 5.4**.

Table 5.3: Results of the water retention tests

Suction (kPa)	Average mass water content (%)		
	Experiments 1 and 2	Experiments 3 and 4	Experiment 5
0 (saturated)	31.38	21.00	30.56
10	19.64	10.26	27.04
20	17.81	9.56	23.97
50	15.20	8.47	19.34
100	14.21	7.56	14.99

Table 5.4: Coefficient of Variability of the water retention tests

Suction (kPa)	Coefficient of Variability (%)		
	Experiments 1 and 2	Experiments 3 and 4	Experiment 5
0 (saturated)	8.38	9.21	6.18
10	19.33	8.55	13.69
20	17.38	7.73	11.47
50	16.84	5.80	5.62
100	17.68	8.57	2.21

The soil-water retention tests revealed that, for Experiments 1 and 2, more soil-water has been retained in the soil matrix compared to experiments 3 and 4. Experiments 3 and 4 revealed a rapid decrease in soil-water between saturation and 10 kPa suction. These trends were expected, since water drained rapidly along large pores of the silty sand.

The rapid decrease in soil-water content between saturation and 10 kPa, observed in Experiments 1 and 2, was not expected, and could have been caused by clay minerals with low water retaining properties. The comparatively higher soil-water retention for experiment 5 was also not expected, but could be attributed to clay minerals with higher water retaining properties.

The soil-water retention properties of the soils tested are characterised by moderate to low variability. This indicates that reasonable estimates of soil water retention characteristics can be obtained from soil-water retention tests.

The results of soil-water retention tests are presented in **Appendix B**.

5.5 Results of the *in situ* tests

5.5.1 Infiltration results

Water content profiles at Experiment 1 were characterised by high water contents in shallow zones and lower water contents in deeper zones. The higher water contents in shallower zones can be attributed to light rainfall during the last few days. Heavy rainfall during the first week of background readings resulted in an increase in water content. The fact that the neutron access holes were installed underneath the tent suggested substantial lateral flow. Neutron access holes 4 and 5 were shielded from lateral flow by the trenches and the empty source hole. Water content values in this area remained low, even at deeper zones.

No significant water content changes at neutron access holes 1, 2 and 3 were observed after the source hole had been filled with water because of a high water content after the rainfall events. Significant water content increases were observed at neutron access hole 5 and, for the deeper zones, at neutron access hole 4.

A high rate of water content increase was observed during the first day. The water level in the source hole was kept at 90 cm. The water level was lowered to 40 cm on the second day, resulting in a lower rate of water content increase. The lower rate of water content increase could be attributed to a lower hydraulic gradient leading to a lower infiltration rate.

Since neutron access holes 4 and 5 were installed at an angle, horizontal distances to the source hole varied at different points of measurement. The shallower the point of measurement, the greater the horizontal distance from the source hole. The fact that the rate of water content increase was approximately the same for all points of measurement, suggests substantial lateral flow.

Complete saturation of the soil matrix was observed in the northern bottom part of the western trench wall. The rest of the wall appeared dry. This saturation was probably caused by preferential flow along plant root holes and fissures (Section 5.6.4).

Experiment 2 was performed after a season of heavy rainfall. The soil-water content was therefore high. Slight rises in water content were observed at shallow and medium depths during the first two days. Water content at a depth of 1.64 m was constant, suggesting near-saturated conditions.

No infiltration tests were conducted during Experiment 3.

Experiment 4 was conducted in the dry season and the original soil water content was therefore low. Complete saturation was reached within 24 hours.

Experiment 5 was conducted after three days of heavy rain. The tent was already erected before the rains came. It was found that the rain had no significant effect on the experiment. Infiltration lasted for two days after which the water was allowed to drain. Neutron probe readings were taken every hour after infiltration commenced and subsequently only four times a day after the first day. Saturation at 0.33 m and 1.13 m was reached after 2 hours and 48 hours respectively.

The first two hours of drainage at 0.33 m and, to a lesser degree, at the other depths could be ascribed to water draining primarily through large pores due to the high degree of saturation. The rate of flow was therefore almost equal to saturated flow. The saturated hydraulic conductivity could be determined by applying the continuity equation during the first two hours of draining.

The continuity equation can be expressed as follows:

$$\frac{d\theta}{dt} = \frac{d}{dz} K(\theta) \frac{dh}{dz} \qquad [5\text{-}10]$$

The hydraulic conductivity over the first two hours of draining was calculated at 1.45×10^{-6} m/s. The infiltration results for Experiment 5 are indicated in **Figure 5.3**.

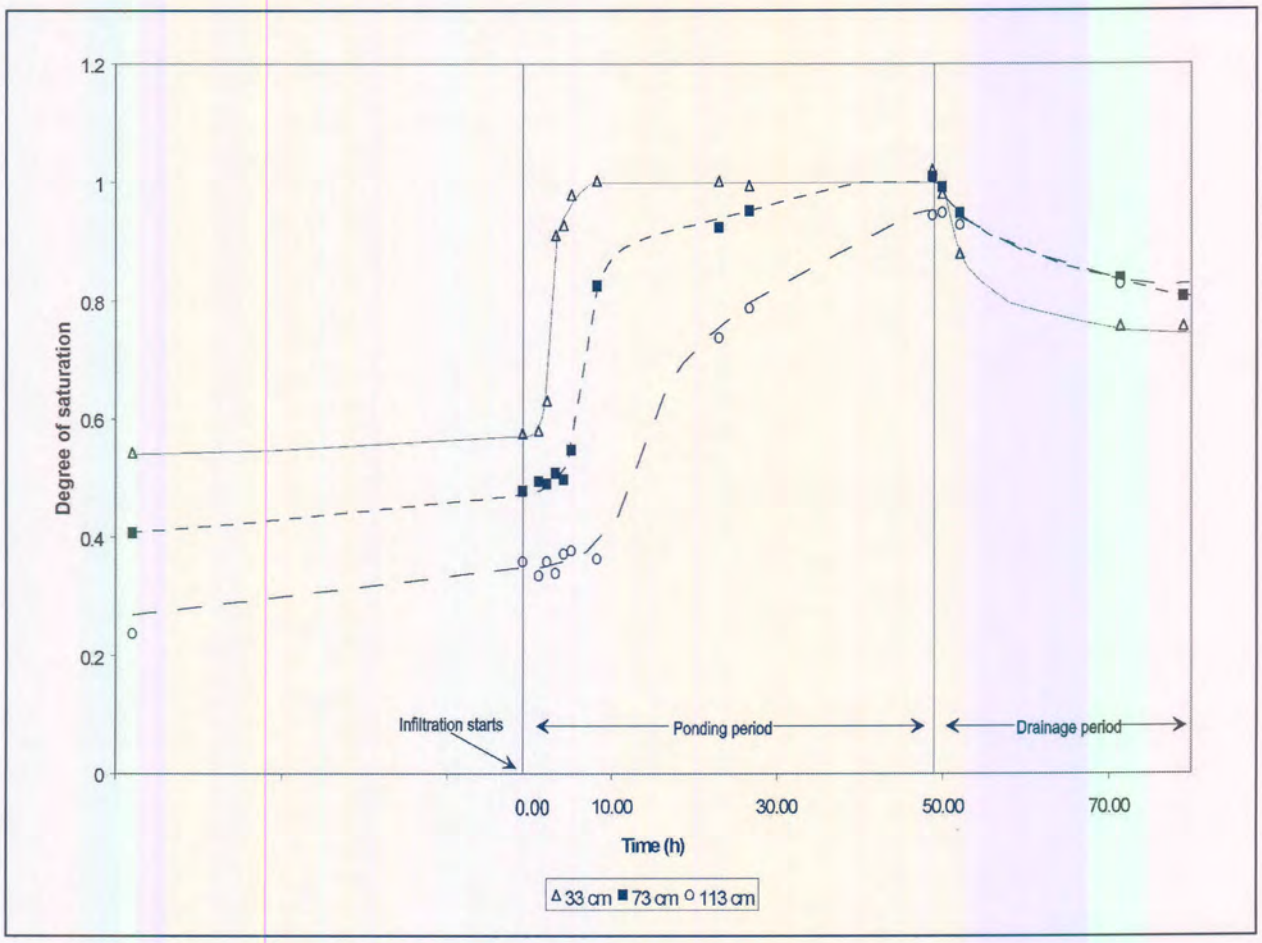

Figure 5.3: Infiltration results at Experiment 5

5.5.2 Results of the Large-Diameter Double-Ring Infiltrometer (LDDRI) tests

The results of the LDDRI tests are summarised in **Table 5.5**.

Table 5.5: Results of the LDDRI tests

	Experiment 2	Experiment 4	Experiment 5
Average hydraulic conductivity (m/s)	2.18×10^{-9}	6.01×10^{-7}	1.91×10^{-6}
Median hydraulic conductivity (m/s)	2.18×10^{-9}	5.59×10^{-7}	1.91×10^{-6}
Coefficient of Variability (%)	N.D.	12.35	15.70
Number of tests	2	5	6

The saturated hydraulic conductivity values, as obtained by the LDDRI tests, are very similar, given the large range of hydraulic heads at which the experiments were conducted. This is confirmed by the low coefficient of variability, which compares well with that of laboratory permeability tests. It also confirms the reliability of LDDRI tests.

5.5.3 Results of the Internal Drainage tests

Two internal drainage tests were conducted during Experiment 2, while one test was conducted during Experiment 4. Curve fitting was conducted by determining the minimum sum of squared residual (SSR) values for the functions. The Generalised Reduced Gradient non-linear optimisation algorithm was applied to determine minimum SSR values, and to determine the values of parameters α and β simultaneously. The results of the internal drainage tests are summarised in **Table 5.6** and in **Figure 5.4**.

Table 5.6: Results of the internal drainage tests

	Experiment 2		Experiment 4
Depth of soil layer, z	0.39	1.14	0.98
Empirical parameter, β	153.716	153.716	102.733
Empirical parameter, α	4.092×10^{-4}	2.017×10^{-2}	1.177×10^{-5}

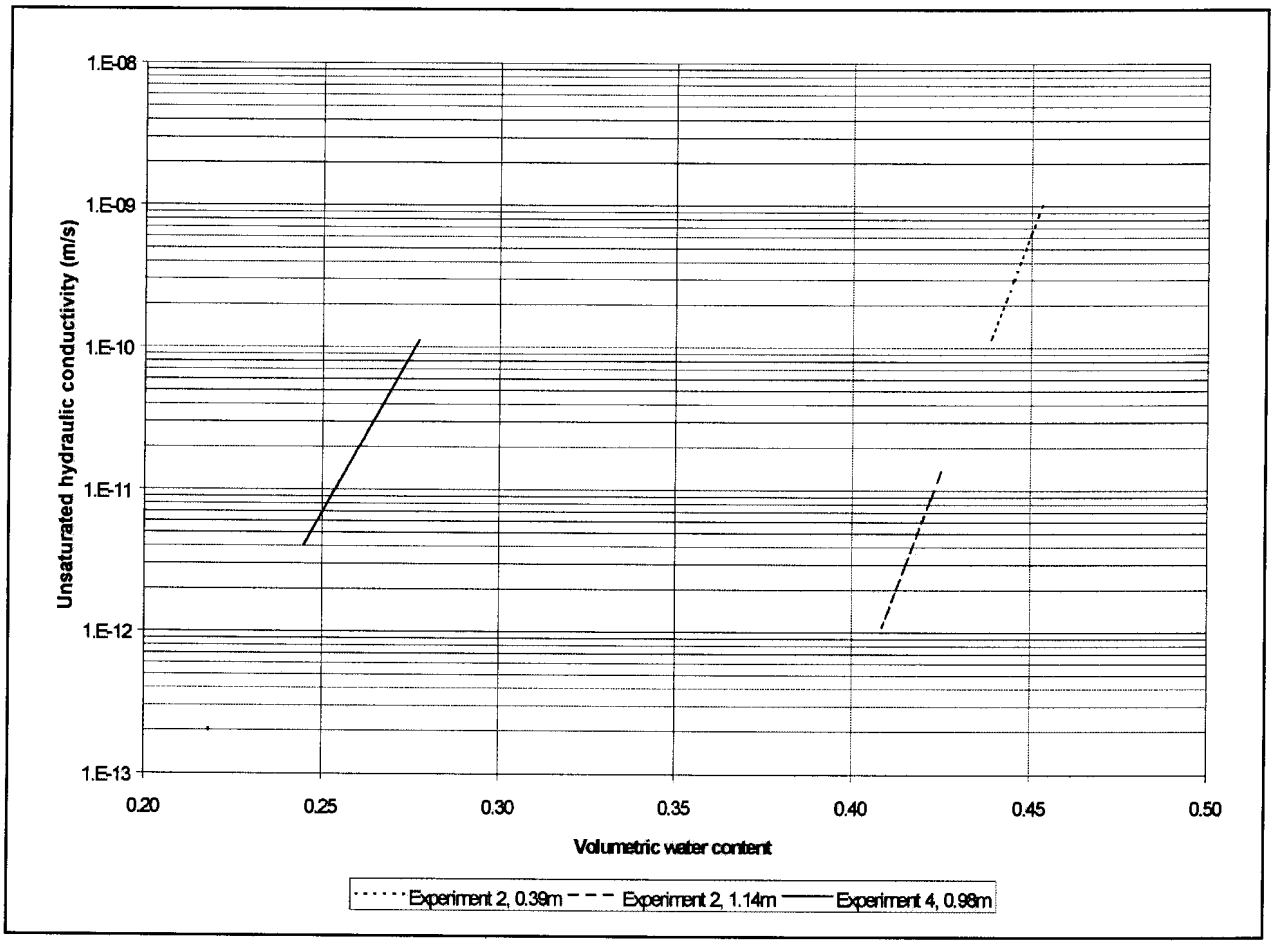

Figure 5.4: Results of the Internal Drainage tests

Equations 5-8 and 5-9 indicate that unsaturated hydraulic conductivity is a function of the empirical parameter β and saturated hydraulic conductivity. The similar parameter β values suggest similar unsaturated hydraulic conductivities for residual soils at depths of 0.39 m and 1.14 m respectively.

The exponential relationship between hydraulic conductivity and water content is in contrast to the typical non-linear sigmoidal relationship generally derived from laboratory and *in situ* tests. This can be ascribed to the form of Equation 5-8, suggesting an exponential relationship.

Because of the simple way in which unsaturated hydraulic conductivity is derived by means of internal drainage methods and the fact that the relationship between soil-suction and water content is ignored, the tests may not yield accurate estimations of unsaturated hydraulic conductivity. In addition, although measurements were taken for more than ten days, little drainage occurred, with the result that unsaturated hydraulic conductivity was derived from a small data range.

5.5.4 Preferential flow

Hydraulic conductivity values derived from laboratory permeability tests were compared with those derived from LDDRI tests. Because of the non-symmetrical shape of the laboratory-determined hydraulic conductivity probability distribution curve and the small amount of data, the effect of preferential flow could not be accurately analysed statistically. However, the effect of preferential flow could be indicated by comparing the median hydraulic conductivity values of the laboratory tests with those of LDDRI tests. The flux increase because of preferential flow is indicated in **Table 5.7**.

Table 5.7: Increase in calculated flux because of preferential flow (hydraulic gradient = 1)

	Experiment 2	Experiment 4	Experiment 5
Median calculated flux of soil matrix (m/s)	7.10×10^{-9}	1.75×10^{-8}	9.80×10^{-7}
Median calculated flux of field soil (m/s)	2.18×10^{-9}	5.59×10^{-7}	1.91×10^{-6}
Calculated factor increase in flux due to preferential flow	None	× 31.9	× 1.95

The variability of hydraulic conductivity should be considered when **Table 5.7** is interpreted. In fact, the hydraulic conductivity of field soils at Experiment 2 is lower than that of the soil matrix. This can be attributed to variable hydraulic conductivity values and subsequent unreliable results. At best, the results proved that preferential flow possibly did not have a significant effect on recharge in field soils at Experiment 2, whereas it possibly had a significant effect on field soils in Experiment 4, while no conclusive evidence was attained that preferential flow had a significant effect on field soils at Experiment 5.

Macropore channelling was observed at Experiment 1. Within 4.5 hours from first filling the source hole, a strong water flow was observed from a plant-root hole, located at the northern bottom part of the western trench wall, 1.97 m deep. The rate of flow was measured at 3×10^{-6} m^3/s. The diameter of the hole was 4 mm. The velocity of water flow can be calculated by means of:

$$v = \frac{q}{A} \qquad [5\text{-}11]$$

where v is the velocity, q is the rate of flow and A is the area perpendicular on water flow. The velocity was therefore calculated at 0.239 m/s.

The preferential flow along plant-root holes and fissures probably caused complete saturation of surrounding soils as was observed at the northern bottom part of the western trench. Water probably flowed into plant-root holes and spread laterally, causing complete saturation of the soil matrix. Flow along fissures was observed in the bottom parts of the western trench. The flow rate could not be measured. Failure of blocks of soil occurred along fissure planes. No other preferential flow was observed in spite of many root-holes along the trench wall.

No preferential flow could be observed at Experiment 2 from the trench wall, excavated near the point of infiltration. The soil was completely saturated. Failure of soil blocks occurred along fissure planes. This suggests preferential flow along these planes.

No preferential flow was observed at Experiment 4 after the inner-ring was filled with water. However, water flow along a plant-root hole was observed within one hour after the inner-ring was filled for the second time. The root hole had a diameter of 5 mm at a depth of 1.10 m. The flow rate was too low to be measured. Within 24 hours, flow along the root hole ceased. No further flow along preferential pathways was observed. The infrequency of flow along the root hole highlighted the dynamic nature of water flow along preferential pathways. The water possibly flushed a soil plug out of its way and water began to flow into the trench. Subsequent transportation of soil particles created another soil plug and water ceased to flow. The complicated nature of water flow can cause difficulties in predicting water flow through macropores.

Tracer tests conducted at Experiment 4 proved that the tracer infiltrated about 15 mm into the soil. The dye was adsorbed strongly by the soil matrix. No macro structures could be identified and no dye was observed along plant-roots, suggesting that no flow of dye took place along preferential pathways.

No preferential flow was observed at Experiment 5.

CHAPTER 6

PREDICTIONS OF GEOHYDROLOGICAL PARAMETERS BASED ON EXPERIMENTAL RESULTS

Based upon data from the literature, the results of laboratory experiments and the results of field experiments, the following correlations were investigated:

- Estimation of porosity from soil profile descriptions, soil-classification tables and empirical equations
- Estimation of saturated hydraulic conductivity from soil profile descriptions, soil-classification tables, empirical equations and soil-water retention characteristics
- Analyses of the various functions describing the soil-water characteristic curve
- Estimation of the unsaturated hydraulic conductivity from empirical equations and soil-water characteristic curves

6.1 Estimations of porosity

Predictions of porosity were made, based on the descriptions of the soil consistency of the various layers at the five experimental sites (Refer to Chapter 4 and Tables 4.1 and 4.2). The predictions of porosity based on soil profile descriptions are summarised in **Table 6.1,** indicating the consistency described for the various horizons.

Table 6.1: Prediction of porosity from soil profile descriptions

Horizon	Description	Predicted porosity	Actual porosity	Prediction
Experiments 1&2				
2	Firm	0.36 – 0.62	0.462	Within range, but wide range of predicted porosity
3	Firm	0.36 – 0.62	0.462	Within range, but wide range of predicted porosity
Experiment 4				
1	Very dense	< 0.34	0.34	Near upper limit
2	Loose	0.40 – 0.45	0.38	Not within range
Experiment 5				
2	Loose	0.40 – 0.45	0.437 – 0.482	Within range, near upper limit
3	Loose	0.40 – 0.45	0.437 – 0.482	Within range, near upper limit
4	Loose	0.40 – 0.45	0.437 – 0.482	Within range, near upper limit

With the exception of the second soil horizon at Experiment 4, accurate predictions of porosity were achieved. However, in the case of Experiments 1 and 2, a wide range of predicted porosity values were suggested, thus rendering predicted values of little use for practical purposes. The wide range was necessary because the consistency of fine-grained soils is influenced by the soil-water content at the time of inspection.

The methods of both Hazen (1930) and Istomina (1957) to predict porosity from the uniformity coefficient were developed for use in uniform soils with little fines. Unfortunately, many of the residual soils that were tested were well-graded with a high percentage of fines. These methods could therefore not be applied in these soils with any accuracy.

Predictions of porosity was made based on the soil textural chart (Schulze, 1995) and these were discussed in Chapter 4. The results are indicated in **Table 6.2**.

Table 6.2: Predicted porosity based on the soil textural chart (Schulze, 1995)

Description	Predicted porosity	Actual porosity	Comment
Experiments 1 and 2			
Silt Loam	0.50-0.53	0.462	Not within range
Silty Clay	0.48	0.462	Near predicted value
Silty Clay Loam	0.47-0.49	0.462	Near lower limit
Experiments 3 and 4			
Sandy Loam	0.47-0.49	0.34-0.38	Not within range
Experiment 5			
Sandy Loam	0.47-0.49	0.437-0.482	Within range

Porosity was under-estimated for most soils, with the exception of sandy loam at experiment 5. In the case of Experiments 1 and 2, the porosity was predicted within 2 to 6 per cent, indicating fairly reliable predictions. Predictions of porosity at experiments 3 and 4 were inaccurate.

6.2 Estimations of saturated hydraulic conductivity

6.2.1 Estimations based on soil profile descriptions and soil classification classes

Saturated hydraulic conductivities were predicted from the soil type description of different residual soils. These predictions were based on the tables compiled by Mathewson (1981). These values were compared to the saturated hydraulic conductivity values, derived from *in situ* LDDRI experiments. The predicted saturated hydraulic conductivity values are summarised in **Table 6.3.**

The measured saturated hydraulic conductivity fell within the predicted range for all residual soils with the exception of the clayey sand of Experiments 3 and 4. A wide range of predicted values is implied for most soil types, especially well-graded sand as found at Experiment 5, thereby significantly limiting its applicability to most hydrogeological investigations.

Table 6.3: Predicted saturated hydraulic conductivity based on soil profile descriptions

Description	Predicted K_s (m/s)	Actual K_s (m/s)	Comment
Experiments 1 and 2			
Silt	$10^{-6} - 10^{-9}$	2.18×10^{-9}	Within range along lower limit
Low plasticity Clay	$10^{-8} - 10^{-11}$	2.18×10^{-9}	Within range
Experiments 3 and 4			
Silty sand	$10^{-6} - 10^{-8}$	5.9×10^{-7}	Within range
Clayey Sand	$10^{-7} - 10^{-9}$	5.9×10^{-7}	Near upper limit
Experiment 5			
Well-graded sand	$10^{-3} - 10^{-7}$	1.91×10^{-6}	Within range, wide range of predicted values

After geotechnical laboratory tests had been conducted on the soil samples, the samples were classified according to the USCS system. Based on this classification, saturated hydraulic conductivities were predicted based on research by Mathewson (1981). The results are summarised in **Table 6.4**:

Table 6.4: Predicted saturated hydraulic conductivity based on USCS soil groups

USCS group	Predicted K_s (m/s)	Actual K_s (m/s)	Comment
Experiments 1 and 2			
CH	$10^{-11} - 10^{-9}$	2.18×10^{-9}	Near upper limit
MH	$10^{-9} - 10^{-7}$	2.18×10^{-9}	Within range along lower limit
Experiment 3 and 4			
SW	$10^{-3} - 10^{-7}$	5.9×10^{-7}	Within range along lower limit
SC	$10^{-7} - 10^{-9}$	5.9×10^{-7}	Near upper limit
Experiment 5			
SC	$10^{-7} - 10^{-9}$	1.91×10^{-6}	Not within range

In general, saturated hydraulic conductivities were not accurately predicted. In the case of CH at Experiment 1 and 2, SC at Experiments 3 and 4 and SC at Experiment 5, saturated hydraulic conductivities were not accurately predicted. In the case of SW at Experiments 3 and 4, a wide range of saturated hydraulic conductivity values were suggested, thereby limiting its applicability in field situations. The reason for these discrepancies can be attributed to the way soil is classified. The USCS system was developed to classify soils according to their geotechnical behaviour, especially with regard to their strength characteristics, not necessarily according to their hydrogeological behaviour. Better predictions of saturated hydraulic conductivity can be derived from soil profile descriptions.

Saturated hydraulic conductivity was predicted based on the soil-textural chart and research by Schulze (1995). The results are indicated in **Table 6.5**.

Table 6.5: Predicted saturated hydraulic conductivity based on the soil textural chart (Schulze, 1995)

Description	Predicted K_s (m/s)	Actual K_s (m/s)	Comment
Experiments 1 and 2			
Silt Loam	1.25×10^{-6} - 2.89×10^{-6}	2.18×10^{-9}	Not within range
Silty Clay	2.50×10^{-7} - 5.56×10^{-8}	2.18×10^{-9}	Near lower limit
Silty Clay Loam	4.17×10^{-7} - $.94 \times 10^{-7}$	2.18×10^{-9}	Not within range
Experiments 3 and 4			
Sandy Loam	1.23×10^{-5} - 7.22×10^{-6}	5.9×10^{-7}	Not within range
Experiment 5			
Sandy Loam	1.23×10^{-5} - 7.22×10^{-6}	1.91×10^{-6}	Near lower limit

The saturated hydraulic conductivity was over-estimated for all soils. In the case of Experiments 1 and 2, saturated hydraulic conductivity was overestimated by a factor of 25 to 1 300. In the case of Experiments 3, 4 and 5, predictions of saturated hydraulic conductivity were more accurate with over-estimations by factors of 4 to 21 recorded. Compared to the results of soil profile descriptions and USCS groups, the values exhibit not as wide range of saturated hydraulic conductivity values and are therefore more reliable.

6.2.2 Empirical equations based on soil fractions

Various empirical equations had been developed (as discussed in Chapter 4) to predict the saturated hydraulic conductivity from sand, silt and clay fractions (soil texture data). In order to assess the reliability of these relationships, the equations have been applied to a wide range of literature-based soil data. A total of 26 data points, representing soils ranging from clay to sand, were applied to the Campbell (1985), Campbell and Shiozawa (1992), and Rawls *et al.* (1982) empirical equations.

In addition, the above-mentioned equations were applied to soil samples obtained from the three experimental sites. The saturated hydraulic conductivity of 13 laboratory samples was determined.

The predicted data were compared to experimentally determined saturated hydraulic conductivity. The results are shown in **Figure 6.1** and the coefficients of correlation are as follows:

Campbell (1985): 0.435

Campbell and Shiozawa (1992): -0.095

Rawls *et al.*(1982): 0.424

Poor correlation coefficients was achieved for the Campbell (1985) and Rawls *et al.* (1982) equations while it appears that no correlation exists in the case of the Campbell and Shiozawa (1992) equation. However, the authors stress the fact that these equations are not valid for all soil types, as confirmed by the results of their investigations.

Better correlation coefficients could be obtained in the case of sand, silty sand and clayey sand, since all these equations have been developed for these soil types. Rawls *et al.* (1982) achieved a correlation coefficient of 0.65 for the soils from which they derived the empirical equation, based on multiple regression techniques. Saturated hydraulic conductivity is greatly influenced by relatively small amounts of silt and clay and the conductivity potential of soils is influenced by the packing and the location of silt and clay in respect of pore connection points.

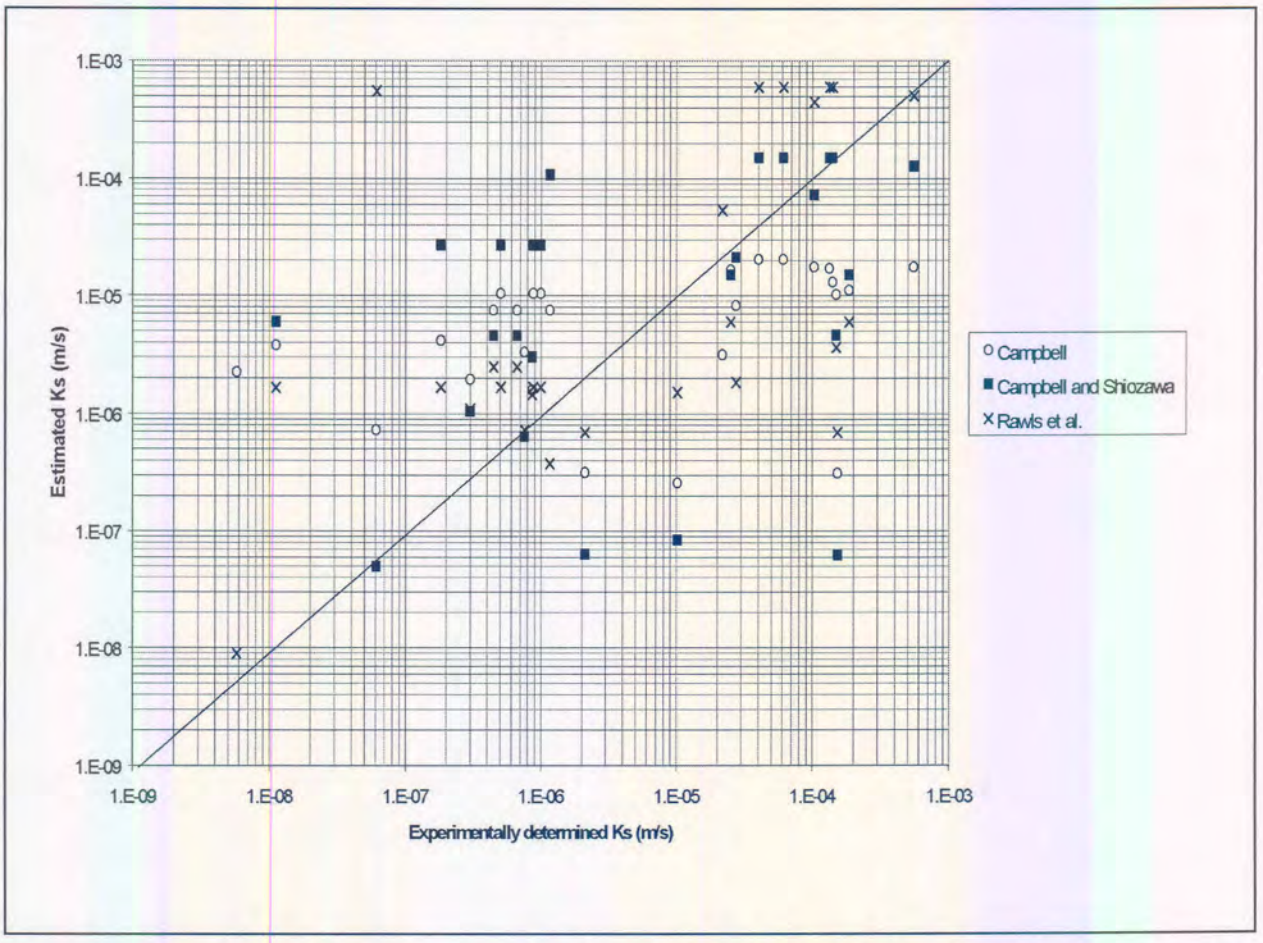

Figure 6.1: Correlation between measured and predicted saturated hydraulic conductivity based on soil fractions

In Chapter 4, it was stated that the parameter, *a*, represents factors such as the shape of grains and grain packing, and this parameter is usually determined from experimental results. Wide ranges of this parameter may indicate inherent inaccuracies of the empirical model. Values of *a* were determined from field experiments and these were compared to the recommended values as derived by the developers of these equations. The results are summarised in **Table 6.6**

Table 6.6: Experimentally derived value and variability of empirical parameter, *a* for popular empirical equations

	Campbell (1985)	Campbell and Shiozawa (1992)	Rawls et al. (1982)
Average value of *a* derived from the experimental sites	2.74×10^{-6}	$5.46 \times ^{-7}$	9.90×10^{-7}
Proposed value for *a*	ND	1.50×10^{-5}	2.78×10^{-6}
Coefficient of variability	114%	126%	120%

Table 6.6 indicates large variations of the empirical parameter, *a*. This indicates that large variations in predicted saturated hydraulic conductivity could occur if the said equations are applied indiscriminately to any soil type. The predicted saturated hydraulic conductivity derived from these equations should therefore be used with caution.

In the case of the Campbell and Shiozawa (1992) equation, the experimentally determined value of parameter *a* differs considerably from that proposed by Campbell and Shiozawa (1992), indicating further

uncertainty about the value of *a*. However, the value proposed by Rawls *et al.* (1982) in their equation is very similar to that determined experimentally, probably indicating a more representative value of *a*.

6.2.3 Empirical equations based on particle-size distribution curves

Literature-based studies

Vukovic and Soro (1992) found that, in the case of fine- to coarse-grained sandy materials, relatively good predictions of saturated hydraulic conductivity could be obtained from the Hazen (1930), Beyer, Sauerbrei and Zunker (Vukovic and Soro, 1992) equations. However, large deviations were recorded in the case of the gravelly sand material, and the equations generally underestimated the saturated hydraulic conductivity. The empirical equations had been developed for sandy materials, characterised by low quantities of fines (generally less than 10 per cent) and a relatively high degree of uniformity (generally less than 5 per cent).

Ten of the fourteen empirical equations under investigation were compared to actual saturated hydraulic conductivity values based on the data from Amer and Awad (1974). In their experiment, Amer and Awad derived an empirical equation from artificially separated soil groups. Basic characteristics of the soil groups are shown in **Table 6.7**. The saturated hydraulic conductivity of each soil group was determined.

Table 6.7: Basic characteristics of the soil groups prepared by Amer and Awad, 1974

	Group 1	Group 2	Group 3	Group 4
d_5 (mm)	0.100 to 0.137	0.171	0.403	0.349 to 0.411
d_{10} (mm)	0.137	0.274	0.460	0.548
d_{17} (mm)	0.137 to 0.141	0.276	0.461	0.553
d_{20} (mm)	0.137 to 0.384	0.438	0.552	0.877
C_u	1 to 21	1 to 5	1 to 5	1 to 4
ε	K determined at 0.293, 0.349, 0.385, 0.411 for each soil group			

The ten empirical equations were applied to each soil group and the saturated hydraulic conductivities were calculated. A large degree of scattering was observed. However, on closer inspection it was observed that some calculated values were strongly correlated to the measured saturated hydraulic conductivity values. A correction factor was calculated for each empirical equation:

$$Correction\ \ factor = \frac{Average\ \ calculated\ \ K}{Experimentally\ \ determined\ \ K} \qquad [6\text{-}1]$$

The correction factor is an indication of the accuracy of the different equations in respect of the different soil groups. A correction factor close to unity indicates accurate predictions of saturated hydraulic conductivity. The correction factors for the ten empirical equations are indicated in **Table 6.8,** varying between 2 and 4 for most equations. The exceptions are the Shahabi *et al.* (1984) and Kenney *et al.* (1984) equations where correction factors of 215 and 22 respectively have been calculated.

Figure 6.2 shows the relationship between experimentally derived and calculated values after the correction factor has been considered. **Figure 6.2** indicates the correlation between calculated and experimentally derived saturated hydraulic conductivity for the ten equations under investigation. In addition, the coefficients of correlation are indicated in **Table 6.8.**

Table 6.8: Correction factors and coefficients of correlation for ten empirical equations

Equation	Correction factor	Coefficient of correlation
Hazen (1930)	3.21	0.7140
Amer and Awad (1974)	1.03	0.9950
Shahabi *et al.* (1984)	215	0.9934
Kenney *et al.* (1984)	22.4	0.8516
Slichter (Vukovic & Soro, 1992)	2.46	0.8701
Terzaghi (Vukovic & Soro, 1992)	2.49	0.8725
Beyer (Vukovic & Soro, 1992)	7.09	0.6099
Sauerbrei (Vukovic & Soro, 1992)	2.93	0.8808
Pavchich (Pravednyi, 1966)	3.89	0.9783
USBR (Vukovic & Soro, 1992)	0.60	0.8119

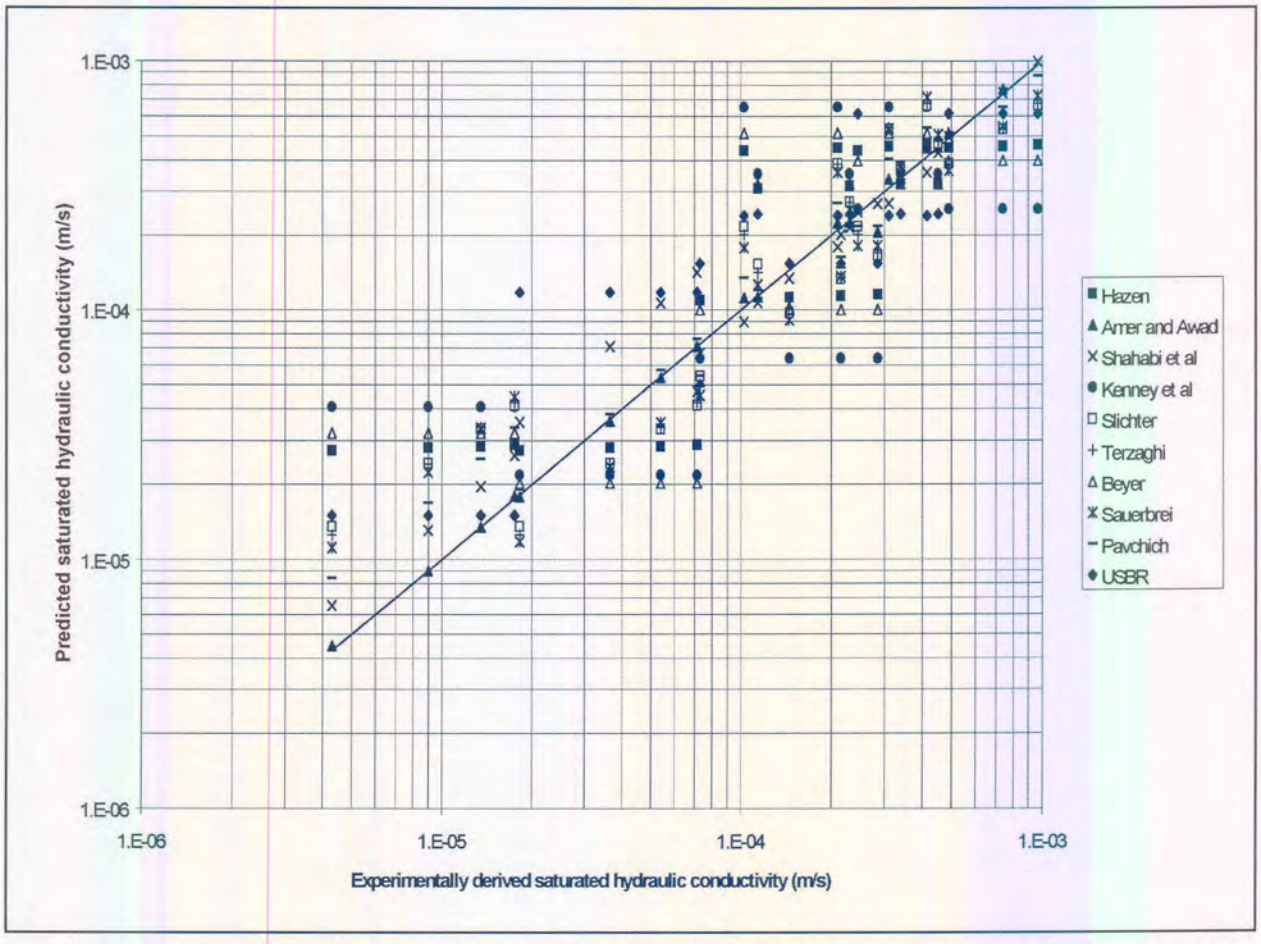

Figure 6.2: Correlation between measured and predicted saturated hydraulic conductivity based on particle size distribution

Equations which incorporate the effect of gradation result in better correlation with saturated hydraulic conductivity. The coefficient of uniformity gives an indication of gradation. The Amer and Awad (1974), Shahabi *et al* (1984), Beyer (Vukovic & Soro, 1992) and Pavchich (Pravednyi, 1966) equations express saturated hydraulic conductivity partly as a function of the coefficient of uniformity. In all of these equations, with the exception of the Beyer equation, a correlation coefficient of more than 0.97 was obtained. The low coefficient of correlation achieved for the Beyer equation could be caused by the fact that the porosity is not considered in this equation.

Experimental studies

Saturated hydraulic conductivity values were derived from the particle-size distributions for residual soils at Experiments 3, 4 and 5. The results of the particle size distributions were applied to ten widely used empirical equations. Predicted saturated hydraulic conductivities were compared to values derived experimentally from *in situ* tests. The results are indicated in **Table 6.9**:

Table 6.9: Predicted saturated hydraulic conductivity for Experiments 3, 4 and 5

Function	Experiment 3 (n=5)		Experiment 5 (n=3)	
	Median K_s (m/s)	Under (-)/Over (+) estimation factor	Median K_s (m/s)	Under (-)/Over (+) estimation factor
Hazen (1930)	2.37×10^{-7}	-2.49	1.25×10^{-7}	-15.23
Amer and Awad (1974)	2.06×10^{-7}	-2.86	2.42×10^{-7}	-7.91
Shahabi *et al* (1984)	4.25×10^{-4}	+721	5.80×10^{-4}	+304
Kenney *et al* (1984)	1.22×10^{-6}	+2.07	1.95×10^{-7}	-9.79
Slichter (Vukovic & Soro, 1992)	1.94×10^{-7}	-3.10	1.91×10^{-7}	-9.98
Terzaghi (Vukovic & Soro, 1992)	1.42×10^{-7}	-3.04	1.99×10^{-7}	-9.59
Beyer (Vukovic & Soro, 1992)	1.42×10^{-7}	-4.17	8.95×10^{-8}	-21.33
Sauerbrei (Vukovic & Soro, 1992)	9.05×10^{-5}	+153	8.71×10^{-5}	+45.6
Pavchich (Pravednyi, 1966)	4.61×10^{-4}	+781	4.29×10^{-4}	+225
USBR (Vukovic & Soro, 1992)	1.95×10^{-5}	+33.07	7.38×10^{-6}	+3.86

The results indicate that large variations (up to a factor of 750) of predicted saturated hydraulic conductivity were obtained. This can be attributed mainly to the fact that all of the developed empirical equations had been developed for uniform sandy soils with little fines. However, in the case of the residual granites investigated, the soils mainly comprise silty, well-graded sand.

Better predictions were derived from the Amer and Awad equation (1974) while the Pavchich (Pravednyi, 1966) and Shahabi *et al.* (1984) equations yielded poor predictions. The poor predictions from the Pavchich equation can be attributed to the fact that the equation had been developed for use in uniform sandy soil and that predicted saturated hydraulic conductivity values are sensitive to the uniformity coefficient.

Average and median predicted saturated hydraulic conductivities, for the ten empirical equations investigated, are indicated in **Table 6.10**. The table indicates that although large variations in predicted saturated hydraulic conductivity were recorded for the various equations, experimentally derived saturated hydraulic conductivity was predicted reasonably accurately for residual soils at Experiments 3 and 4. The large variation in predicted saturated hydraulic conductivity suggests that soil properties other than particle-size distribution and porosity could cause an uncertainty of up to two orders of magnitude for predicted saturated hydraulic conductivity. However, the large variations can also be attributed to the equations' inability to accurately predict saturated hydraulic conductivity as a function of particle-size distribution for a wide range of soil types.

Table 6.10: Predicted saturated hydraulic conductivity for Experiments 3, 4 & 5 based on ten empirical functions

	Experiment 3 & 4	Experiment 5
Average K_s (m/s) (All functions)	1.16×10^{-4}	1.09×10^{-4}
Median K_s (m/s) (All functions)	6.27×10^{-7}	2.73×10^{-7}
***In situ* determined K_s (m/s)**	5.90×10^{-7}	1.91×10^{-6}
Over (+)/under (-) estimation of K_s	+ 2.78	- 7.71
Coefficient of variability (%)	200.8	199.9

As is the case with equations predicting saturated hydraulic conductivity from soil fractions, the generic empirical equation can be expressed as:

$$K_s = a_{gsd} \cdot f(D_e, C_u, \varepsilon) \qquad [6\text{-}2]$$

where D_e, C_u and ε represent effective grain diameter, uniformity coefficient and porosity respectively. The parameter a_{gsd} is a constant and reflects factors other than particle-sizes with an effect on saturated hydraulic conductivity such as the shape of the grains and packing. It is related to the parameter a of empirical equations based on soil fractions. The parameter, a_{gsd}, is derived experimentally and wide ranges of the value could reflect inherent errors regarding the empirical function. In these cases, the parameter will not be a constant, but will vary according to different soil types. The more parameter a_{gsd} varies with regard to different soil types, the greater the inherent errors of the empirical equation.

Table 6.11 indicate the value of parameter a_{gsd} as indicated in literature (a_{gsd}), derived from experiments by Amer and Awad (1974) (a_{gsd1}) and from data collected at Experiments 3 and 5 respectively (a_{gsd3} and a_{gsd5}).

Table 6.11: Experimentally derived values of parameter a_{gsd}

	a_{gsd}	a_{gsd1}	a_{gsd3}	A_{gsd5}	Coefficient of variation
Hazen (1930)	4.72×10^{-9}	1.47×10^{-9}	1.17×10^{-8}	7.19×10^{-8}	147.97
Amer and Awad (1974)	9.54×10^{-9}	9.54×10^{-9}	2.73×10^{-8}	7.54×10^{-8}	102.69
Shahabi *et al* (1984)	1.20×10^{-6}	5.59×10^{-9}	1.66×10^{-9}	3.95×10^{-9}	197.53
Kenney *et al* (1984)	5.00×10^{-8}	2.24×10^{-9}	2.42×10^{-8}	4.90×10^{-7}	164.57
Slichter (Vukovic & Soro, 1992)	1.04×10^{-7}	4.21×10^{-8}	3.21×10^{-7}	1.04×10^{-6}	121.35
Terzaghi (Vukovic & Soro, 1992)	5.00×10^{-2}	2.01×10^{-2}	1.52×10^{-1}	4.80×10^{-1}	119.94
Beyer (Vukovic & Soro, 1992)	4.62×10^{-9}	6.51×10^{-10}	1.92×10^{-8}	9.84×10^{-8}	149.15
Sauerbrei (Vukovic & Soro, 1992)	3.58×10^{-8}	1.22×10^{-8}	2.33×10^{-10}	7.85×10^{-10}	135.75
Pavchich Pravednyi, 1966)	3.58×10^{-9}	9.20×10^{-9}	4.58×10^{-11}	1.59×10^{-10}	149.42
USBR (Vukovic & Soro, 1992)	4.92×10^{-10}	8.22×10^{-10}	1.49×10^{-11}	1.27×10^{-10}	100.79

Table 6.11 shows that the value of parameter a_{gsd} varies greatly for all empirical equations investigated. It indicates that the equations may not be suitable to accurately predict the saturated hydraulic conductivity. The equations showing the least variation are the USBR (Vukovic & Soro, 1992) and Amer and Awad (1974) equations. It indicates that these equations probably offer the most reliable method for predicting saturated hydraulic conductivity for the soils tested. However, these equations still result in highly variable predictions of saturated hydraulic conductivity that may vary by up to one order of magnitude. The equations showing the highest variation include the Shahabi *et al.* (1984) and Kenney *et al* (1984) equations. However, with regard to the Shahabi *et al.* (1984) equation, where the value of parameter a_{gsd} has been derived experimentally from data of Amer and Awad (1974), Experiment 3 and Experiment 5 differ remarkably from those proposed in literature. An incorrect value of a_{gsd} could possibly have been quoted in the literature.

Experimental studies: Fine-grained soils

Saturated hydraulic conductivity is predicted on the basis of the Atterberg limits by applying the method proposed by Tavenas *et al.* (1983a). This method is described in Chapter 4. Because the method is only valid for fine-grained soils, i.e. soils with significant clay content, it was only applied for residual soils at Experiments 1 and 2. The parameter, I_c, a function of both clay content and total PI, was determined for eight soil samples. With the void ratio known, the values were plotted on the diagram as proposed by Tavenas *et al.* and are shown in **Figure 6.3** indicating predicted saturated hydraulic conductivity. The parameter, I_c, and the predicted saturated hydraulic conductivity were statistically analysed and are shown in **Table 6.12**.

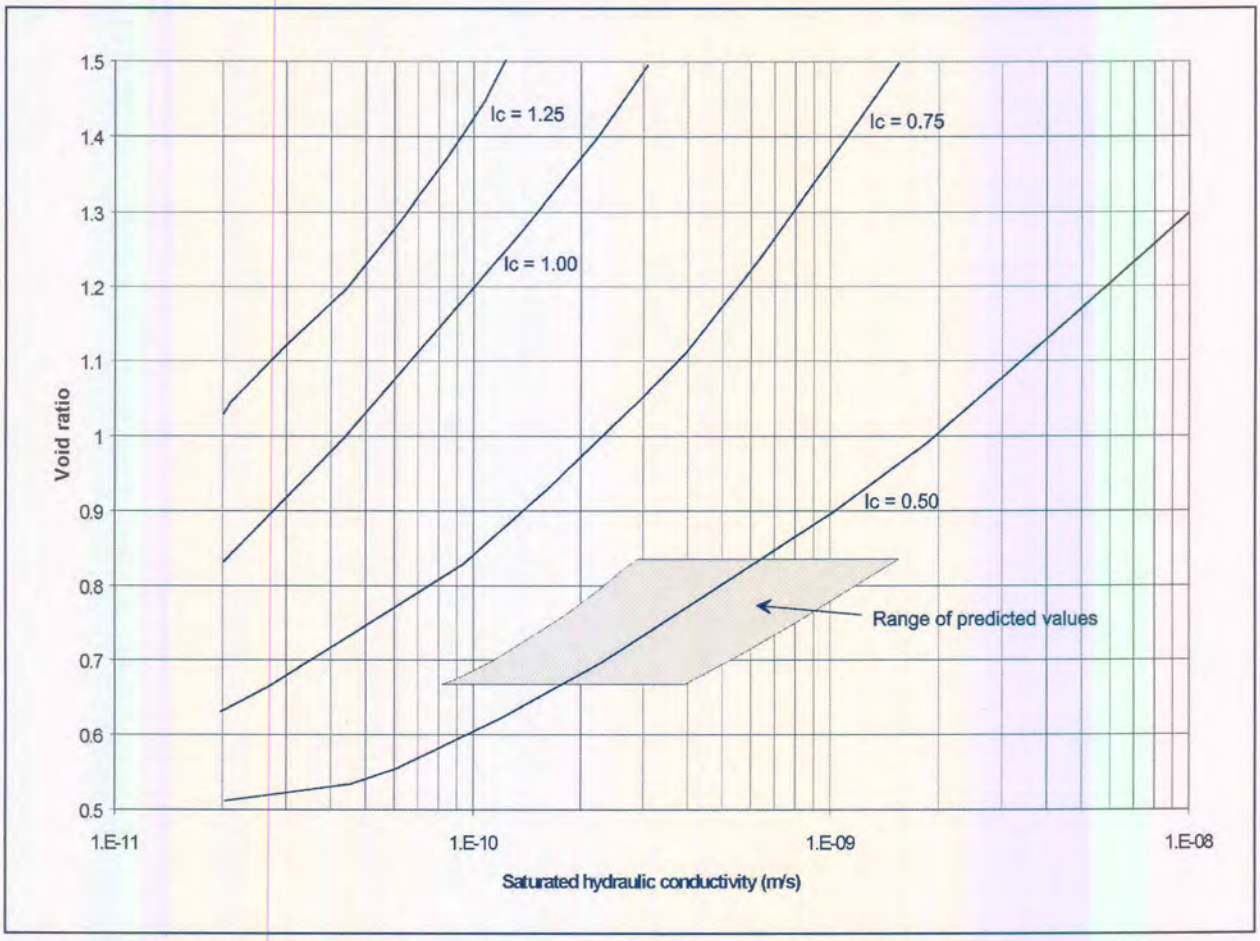

Figure 6.3: Predicted saturated hydraulic conductivity based on Atterberg limits

Table 6.12: Statistical analysis of predicted saturated hydraulic conductivity and parameter, I_c

		Saturated hydraulic conductivity (m/s)	Parameter I_c
Predicted values	Average	7.35×10^{-10}	0.51
	Median	8.05×10^{-10}	0.54
	Maximum	$>1.00 \times 10^{-9}$	0.63
	Minimum	3.70×10^{-10}	0.33
	Coefficient of variation (%)	39.24	21.90
In situ derived median value		2.18×10^{-9}	NA
Sample size		8	8

Predicted saturated hydraulic conductivity values compare well with experimentally derived saturated hydraulic conductivity values as determined by LDDRI tests. The saturated hydraulic conductivity was under-estimated by a factor of about three, which is acceptable, given the large natural spatial variation of saturated hydraulic conductivity. In addition, the variation of predicted saturated hydraulic conductivity is acceptable and compares well with other predictive techniques. The variation of predicted saturated hydraulic conductivity values is similar to the variation of the parameter, I_c, for the eight soil samples analysed.

6.2.4 Predictions of saturated hydraulic conductivity based on soil-water retention data

Various empirical equations have been developed to estimate the saturated hydraulic conductivity from water retention data. These equations were discussed in Chapter 4. In order to assess the reliability of these relationships, the equations were applied to a wide range of literature-based soil data. The data used in the analysis of empirical equations related to soil fraction were also used in this analysis. A total of 26 data points, representing soils ranging from clay to sand, were applied to the Ahuja *et al.* (1985) equation. A correlation coefficient of –0.00165 was achieved, indicating very poor relationship.

In addition to the Ahuja *et al.* (1985) equation, the Brutsaert (1967) and Campbell (1985) equations were applied to five soil types, ranging from sand to clay. The Brooks and Corey (1964) equation was applied to water retention data for the five soil types and the Brooks and Corey pore-size index, residual water content and air-entry values were determined by non-linear regression techniques. These parameters were applied to the Brutsaert (1967) and Campbell (1985) equations and the saturated hydraulic conductivity was determined.

The results indicate very poor correlation between water retention data and saturated hydraulic conductivity, and correlation coefficients of –0.05 and –0.096 respectively were achieved for the Brutsaert (1967) and Campbell (1985) equations.

6.3 Description of the soil-water characteristic curve

Several mathematical functions had been developed to describe the soil-water characteristic curve and these were discussed in Chapter 4. The indirect determination of unsaturated hydraulic conductivity entails integration of these functions. The various models developed to determine unsaturated hydraulic conductivity were also discussed in Chapter 4. Reliable estimations of unsaturated hydraulic conductivity are only possible on condition that these mathematical functions accurately describe the soil-water characteristic curve. Since the soil-water characteristic curve could be either exponential or sigmoidal in shape (depending on the type of soil), the development of a single function that is valid for all soil-water characteristic curve shapes is difficult.

Four popular functions, which describe the soil-water characteristic curve, were tested for five different soil types. The functions applied were:

- The Gardner (1958) function
- The Brooks and Corey (1964) function
- The Van Genuchten (1980) function
- The Fredlund and Xing (1994) function

These functions were applied to soil-water retention data obtained from the literature. Five data sets were selected for further analysis, namely:

- Sand consisting of 0.5 mm to 0.25 mm sand fraction as prepared by Childs and Collis-George (1950) as part of their research for the development of the Childs and Collis-Geoge model to derive unsaturated hydraulic conductivity from soil-water retention data
- Fine sand consisting of soil with grain sizes ranging from 0.8 to 0.05 mm (Vachaud, Gandet & Kuraz, 1974)
- Silty clayey sand (sandy loam) as Elzeftawy and Dempsey (1976) used in their research on steady state-flow in materials for subgrade layers on roads
- Sandy clay-silt (Guelph loam) from the research conducted by Elrick and Bowman (1964)
- Clay consisting of soil with a clay percentage greater than 48 from the research of Neuman, Feddes & Besler (1974)

Curve fitting was conducted by determining the minimum total of squared residual (SSR) values for the functions. The Generalised Reduced Gradient non-linear optimisation algorithm was applied to determine minimum SSR values. The results compared well to curve fitting by applying the Marquardt-Levenberg non-linear optimisation algorithm. Both algorithms required initial values in order to determine optimum parameter values. These values were obtained by trial and error.

The results of the curve fitting are presented in **Figures 6.5** to **6.9** and in **Table 6.13**. Good fit is represented by low SSR values. In addition, correlation coefficients were determined to confirm good fit. SSR values were determined for low, medium and high volumetric water contents to assess the reliability of the functions over the entire soil-water retention range.

Table 6.13: Correlation between experimentally derived soil-water characteristic curves and their related functions

Soil type	Function	SSR at degree of saturation percentages				R^2
		(30%)	(60%)	(90%)	Entire range	
Sand	Gardner (1958)	5.32E-05	2.21E-05	1.65E-04	4.04E-03	0.99190
	Brooks and Corey (1964)	2.36E-05	1.85E-05	3.41E-02	1.89E-04	0.98543
	Van Genuchten (1980)	3.78E-04	5.00E-05	2.21E-05	2.29E-03	0.99657
	Fredlund and Xing (1994)	1.65E-05	5.04E-05	7.66E-06	3.83E-04	0.99923
Fine Sand	Gardner (1958)	3.37E-05	5.15E-05	8.60E-06	4.43E-04	0.99899
	Brooks and Corey (1964)	4.39E-06	1.79E-04	3.66E-02	9.42E-04	0.90465
	Van Genuchten (1980)	1.14E-05	3.03E-05	1.39E-06	2.38E-04	0.99947
	Fredlund and Xing (1994)	3.99E-05	3.77E-05	8.73E-07	5.10E-04	0.99896
Silty-clayey sand	Gardner (1958)	2.09E-05	1.81E-05	1.93E-05	3.89E-04	0.98710
	Brooks and Corey (1964)	1.16E-05	1.63E-04	1.73E-06	4.45E-04	0.98476
	Van Genuchten (1980)	1.97E-05	1.85E-05	2.10E-05	3.54E-04	0.98817
	Fredlund and Xing (1994)	2.31E-05	3.31E-05	2.13E-05	3.59E-04	0.98805
Sandy silt-clay	Gardner (1958)	3.28E-03	1.11E-03	3.23E-02	6.73E-02	0.94548
	Brooks and Corey (1964)	1.26E-05	1.13E-04	1.61E-05	4.31E-04	0.99927
	Van Genuchten (1980)	6.24E-08	4.59E-05	4.66E-05	4.29E-04	0.99928
	Fredlund and Xing (1994)	4.27E-04	2.97E-05	1.31E-03	3.22E-03	0.99518
Clay	Gardner (1958)	3.40E-04	3.64E-05	2.28E-06	1.61E-03	0.99836
	Brooks and Corey (1964)	3.42E-07	4.17E-05	3.25E-04	1.33E-03	0.97117
	Van Genuchten (1980)	7.20E-06	1.97E-04	1.07E-04	6.86E-04	0.99923
	Fredlund and Xing (1994)	1.60E-04	5.20E-05	4.07E-05	5.69E-04	0.99938
Ave-rage	Gardner (1958)	7.45E-04	2.48E-04	6.50E-03	1.48E-02	0.98437
	Brooks and Corey (1964)	1.05E-05	1.03E-04	1.42E-02	6.67E-04	0.96906
	Van Genuchten (1980)	8.34E-05	6.84E-05	3.96E-05	7.99E-04	0.99654
	Fredlund and Xing (1994)	1.33E-04	4.06E-05	2.75E-04	1.01E-03	0.99616

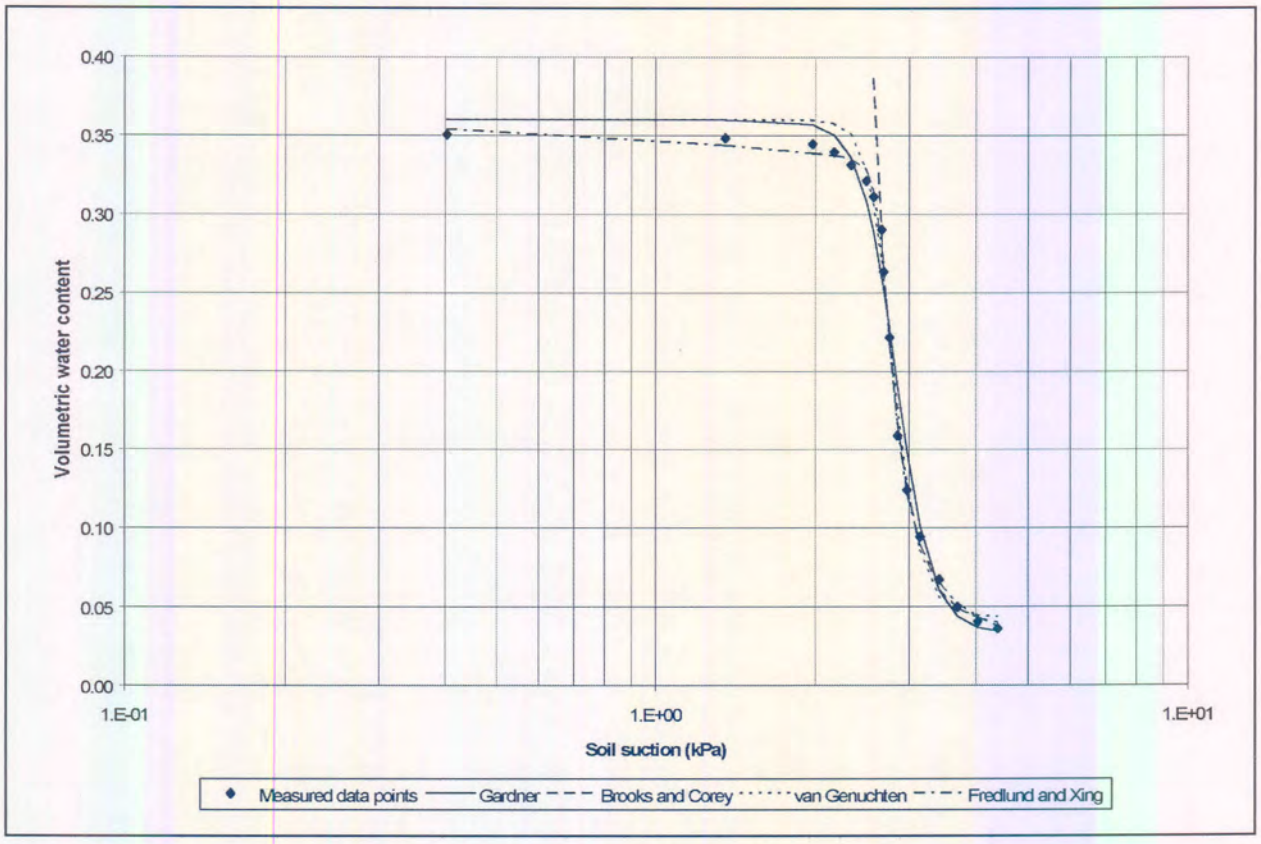

Figure 6.4: Description of the soil-water characteristic curve for sand

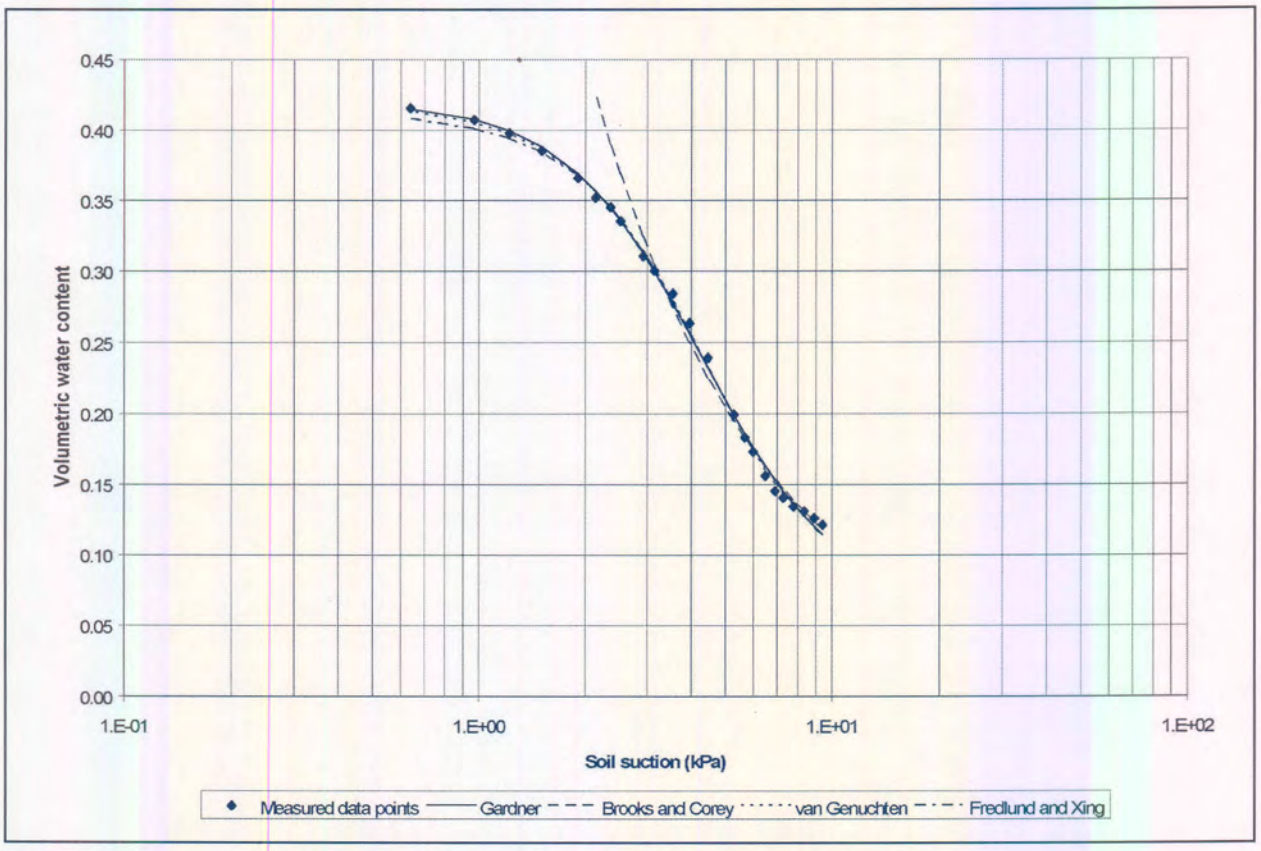

Figure 6.5: Description of the soil-water characteristic curve for fine sand

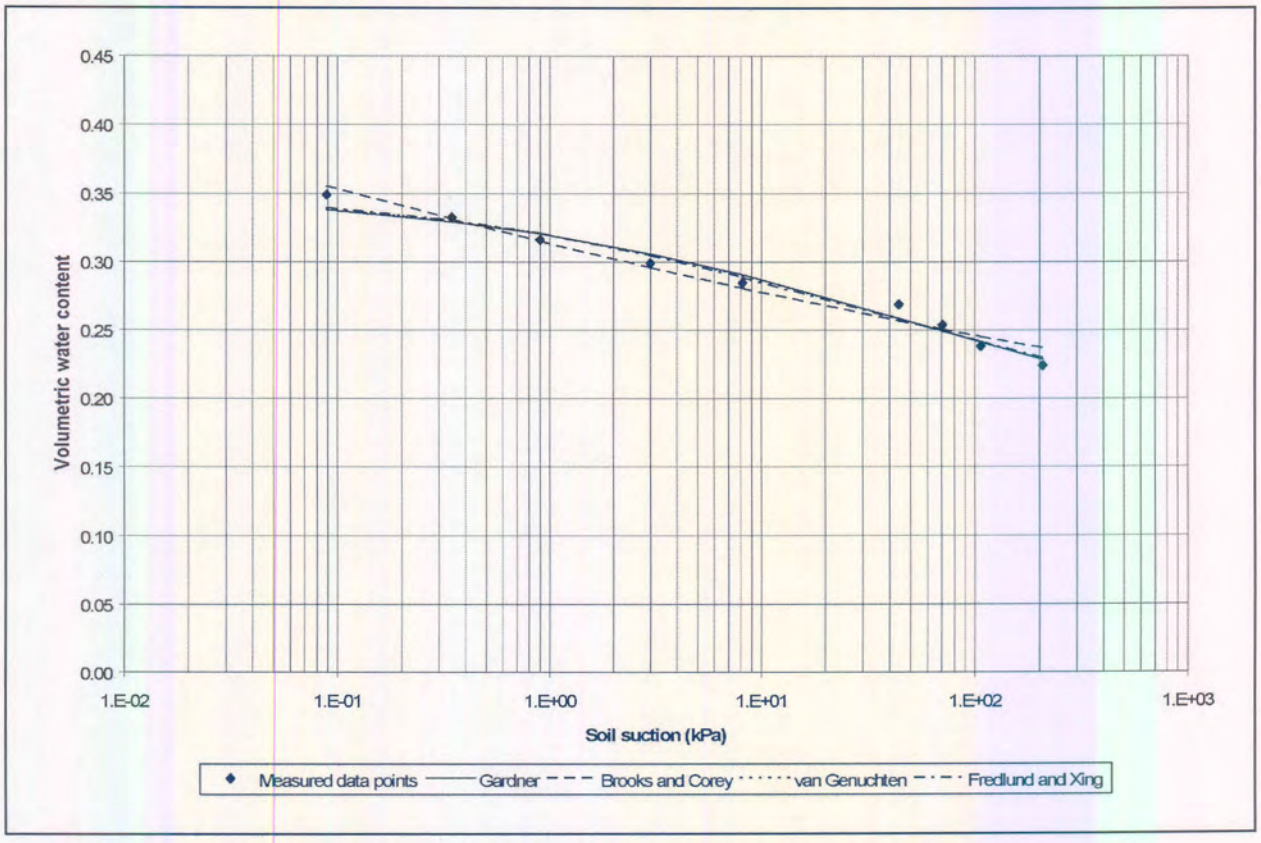

Figure 6.6: Description of the soil-water characteristic curve for silty clayey sand

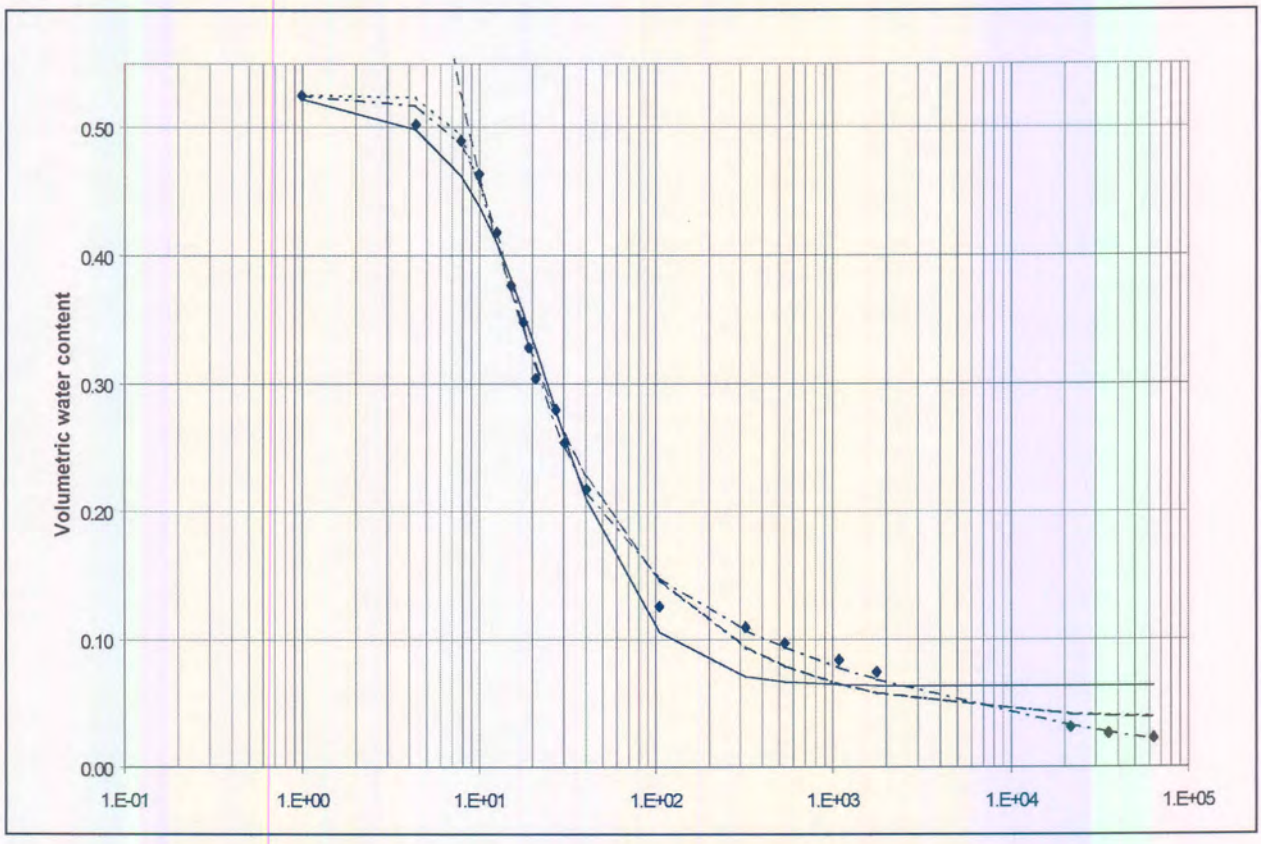

Figure 6.7: Description of the soil-water characteristic curve for sandy silt-clay

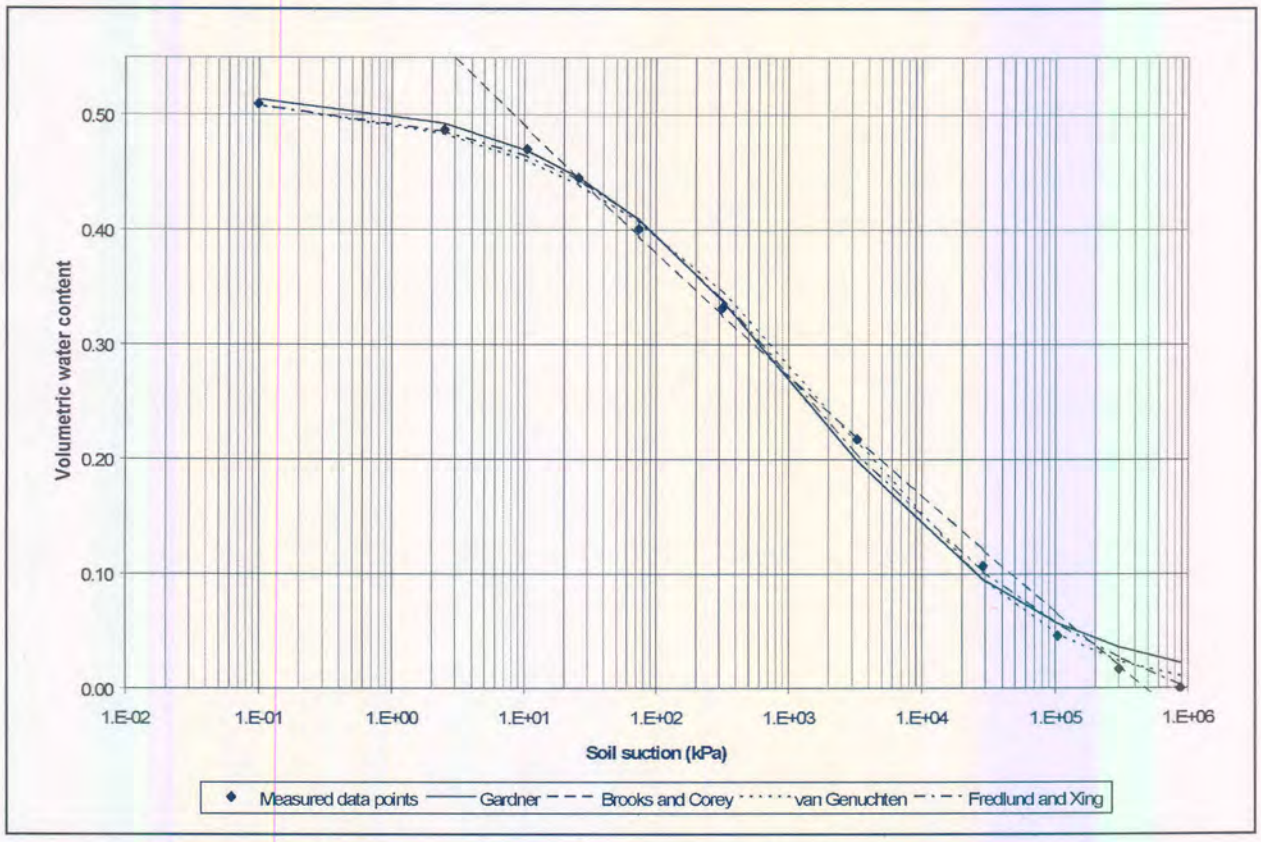

Figure 6.8: Description of the soil-water characteristic curve for clay

Good results were obtained for the four functions applied to the various soil-water retention data sets. Correlation coefficient values ranged from 0.99947 in the case of the Van Genuchten (1980) function applied to soil-water retention data for fine sand to 0.90465 in the case of the Brooks and Corey (1964) function applied to soil-water retention data for fine sand. The Gardner (1958), Van Genuchten (1980) and Fredlund *et al.* (1994) functions best describes sigmoidally shaped soil-water characteristic curves, while the Brooks and Corey (1964) function best describes exponentially shaped soil-water characteristic curves.

The Brooks and Corey (1964) model requires the air-entry value to be known in order to accurately describe the soil-water characteristic curve. Although the air-entry value is difficult to determine experimentally, it can be estimated from initial hand-drawn soil-water characteristic curves.

Good fit was obtained for all five soil-water retention data-sets. The high dependency values between the parameters *m* and *n* in both the Van Genucten (1980) and Fredlund *et al.* (1994) functions suggest that three parameters are probably adequate to describe most soil-water characteristic curves. This is confirmed by the good results obtained from both the Gardner (1958) and Brooks and Corey (1964) functions that only apply three parameters to describe the soil-water characteristic curve. Good results were also obtained by placing a restriction on the *m* parameter of the Van Genucten (1980) function by expressing it as a function of the parameter *n,* and thereby expressing the soil-water characteristic curve in terms of three unknown parameters. The restriction was necessary to obtain a closed function in order to estimate the unsaturated hydraulic conductivity. However, rather poor fit was obtained in the case of sandy silt-clay, as described by the Gardner (1958) function. This can be ascribed to the exponential shape of the specific soil-water characteristic curve while the Gardner (1958) function was developed to describe sigmoidally shaped soil-water characteristic curves. In contrast, best fit was derived by the Brooks and Corey (1964) function, developed to describe mainly exponentially shaped curves. The Brooks and Corey (1964) function was less accurate in estimating soil-water retention at higher suction values. The Brooks and Corey (1964) functions apply two functions to describe the soil-water

characteristic curve, depending on the air-entry value. This results in a kink in the curve at high soil suction levels, inconsistent with experimental data.

6.4 Estimation of the soil-water characteristic curve

6.4.1 Soil fractions

Soil water retention properties can be predicted from soil fractions, based on the methods proposed by Gupta and Larson (1979). This method was discussed in Chapter 4. Volumetric water contents were predicted at a number of soil suction values. These values were compared with measured soil-water characteristic curves as obtained from laboratory water retention tests. The results are presented in **Table 6.14** and **Figures 6.10** to **6.12.**

Table 6.14: Measured and predicted water content at six soil suction values

Soil suction (kPa)	Volumetric water content					Coefficient of variability (%)
	Measured	Average predicted	Median predicted	Maximum predicted	Minimum predicted	
Experiments 1 and 2						
4	0.331	0.482	0.490	0.492	0.456	3.58
10	0.283	0.430	0.441	0.444	0.396	5.35
33	0.237	0.386	0.399	0.412	0.335	8.94
60	0.218	0.365	0.379	0.396	0.308	10.75
100	0.202	0.348	0.361	0.382	0.287	12.07
1000	0.142	0.284	0.297	0.322	0.218	16.02
Experiments 3 and 4						
4	0.206	0.235	0.239	0.252	0.211	7.04
10	0.181	0.179	0.186	0.196	0.151	11.05
33	0.157	0.148	0.147	0.181	0.119	16.51
60	0.145	0.140	0.136	0.179	0.112	19.10
100	0.136	0.134	0.127	0.177	0.106	21.03
1000	0.095	0.106	0.095	0.155	0.082	28.27
Experiment 5						
4	0.428	0.347	0.350	0.354	0.338	2.39
10	0.396	0.271	0.275	0.278	0.260	3.53
33	0.318	0.205	0.209	0.210	0.194	4.49
60	0.266	0.178	0.183	0.183	0.168	4.93
100	0.222	0.159	0.163	0.164	0.149	5.31
1000	0.086	0.102	0.105	0.108	0.094	7.16

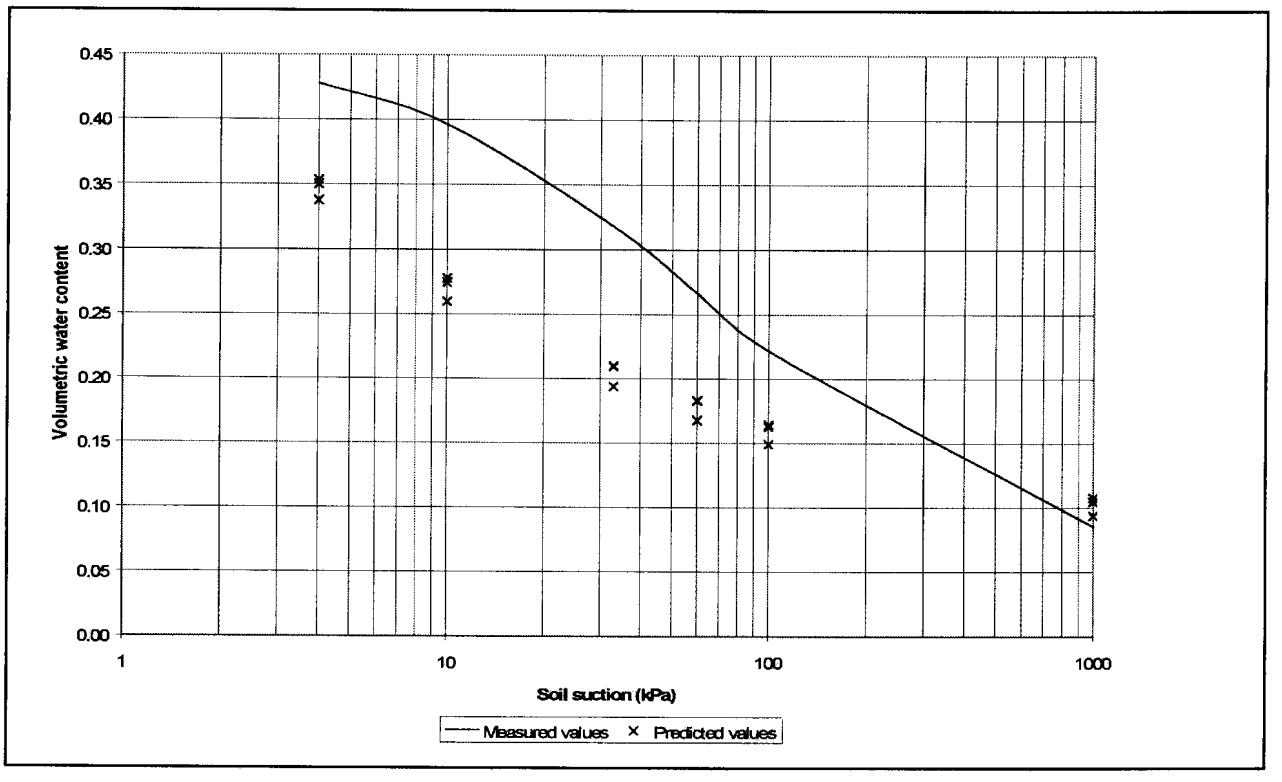

Figure 6.9: Correlation between the measured and predicted soil-water characteristic curve at Experiment 2

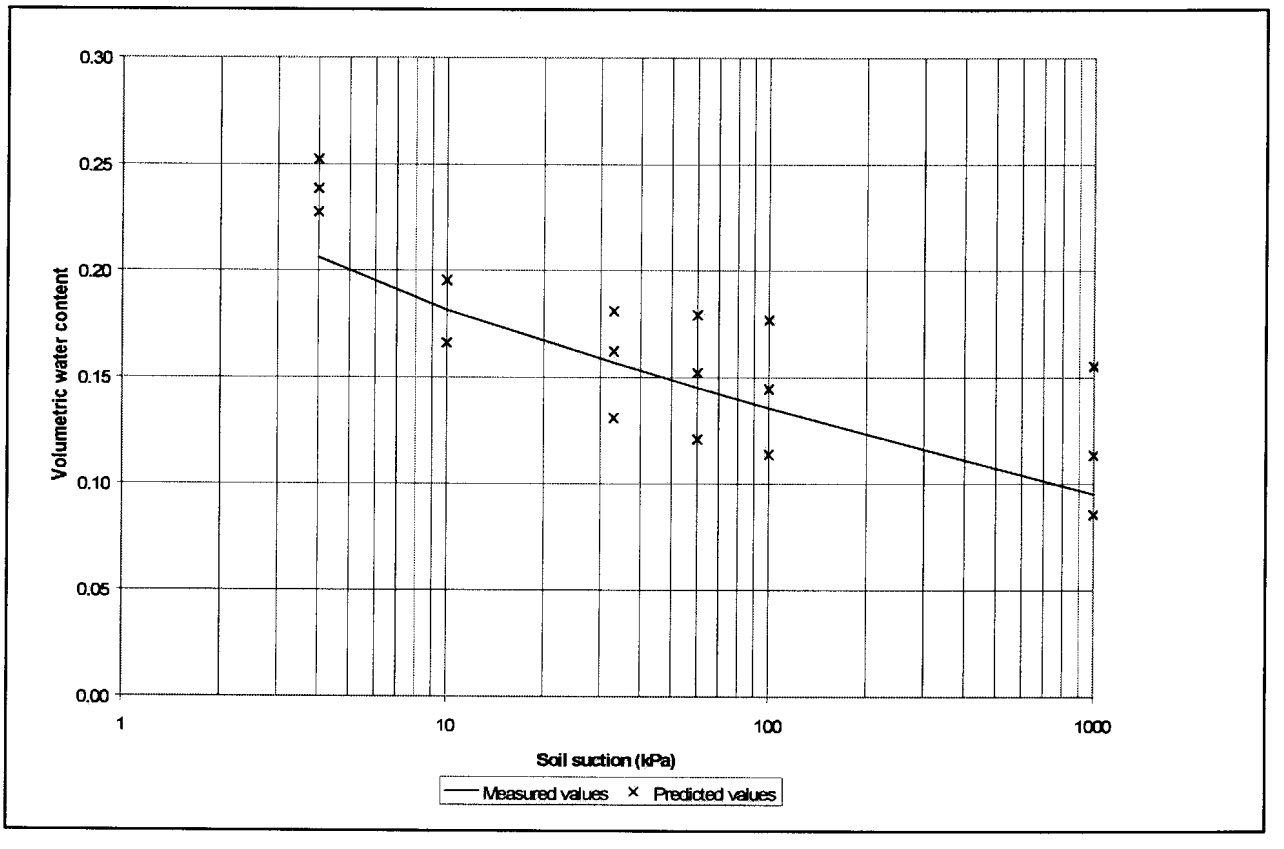

Figure 6.10: Correlation between the measured and predicted soil-water characteristic curve at Experiment 4

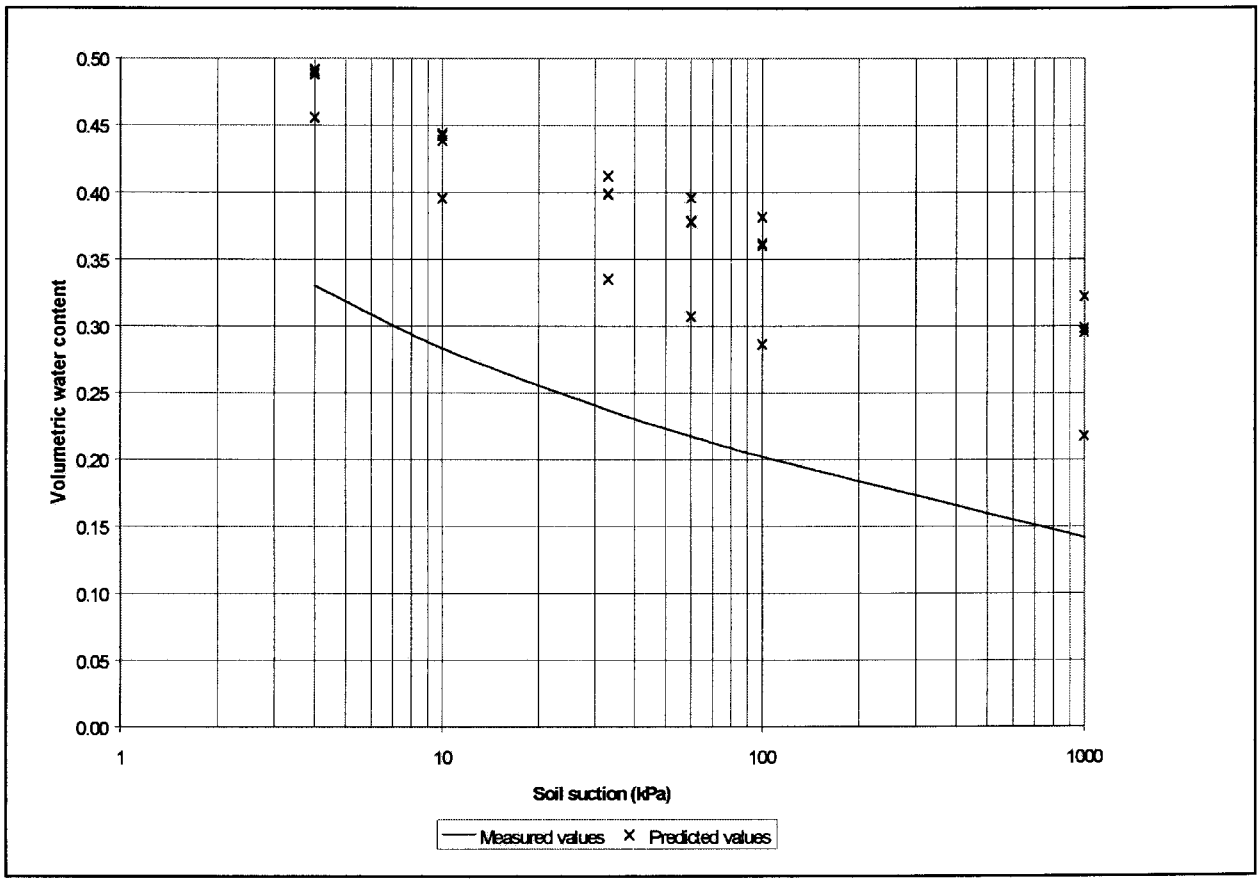

Figure 6.11: Correlation between the measured and predicted soil-water characteristic curve at Experiment 5

Table 6.14 and **Figures 6.10** to **6.12** indicate that in the case of Experiments 3 and 4, the soil-water characteristic curve has been accurately predicted by the Gupta and Larson (1979) regression model. However, less accurate predictions of soil-water characteristic curves were achieved in the case of Experiments 1 and 2 and Experiment 5. This may be caused by the high porosity values of residual soils at Experiments 1, 2 and 5. It appears that the porosity value has a significant effect on soil-water characteristic curves.

6.5 Estimation of unsaturated hydraulic conductivity

6.5.1 Statistical equations

The Van Genuchten (1980) and Fredlund *et al.* (1994) models were applied to estimate unsaturated hydraulic conductivity as a function of volumetric water content. These results were compared to measured unsaturated hydraulic conductivity as obtained from literature.

Soil-water retention data-sets of the five soils referred to in Section 6.4 were fitted to the Van Genuchten (1980) and Fredlund and Xing (1994) functions. In order to obtain a closed-form equation, a restriction was placed on the parameter, *m,* of the Van Genucten (1980) model in terms of:

$$m = 1 - \frac{1}{n} \qquad [6\text{-}3]$$

This resulted in a slight loss of flexibility regarding the Van Genucten (1980) function. However, good fit was obtained when the aid restriction was applied. When the Mualem (1976) model for estimating unsaturated hydraulic conductivity, is applied, unsaturated hydraulic conductivity can be expressed as:

$$K(\psi)=\frac{K_s\left\{1-(\alpha\psi)^{mn}\left[1+(\alpha\psi)^n\right]^{-m}\right\}^2}{\left[1+(\alpha\psi)^n\right]^{m\ell}} \qquad \text{where} \qquad m=1-1/n \qquad [6\text{-}4]$$

Since the volumetric water content is a function of soil suction, unsaturated hydraulic conductivity can be expressed as a function of volumetric water content. The parameter l had been defined as the pore connectivity factor, where Mualem (1976) has suggests a value equal to 0.5.

Fredlund *et al.* (1994) maintain that, by applying the model of Childs and Collis-George (1950) to the Fredlund and Xing (1994) function, unsaturated hydraulic conductivity can be expressed as:

$$K_r(\psi)=\Theta^q(\psi)\frac{\int_{\ln(\psi)}^{b}\frac{\theta(e^y)-\theta(\psi)}{e^y}\theta'(e^y)dy}{\int_{\ln(\psi_a)}^{b}\frac{\theta(e^y)-\theta_s}{e^y}\theta'(e^y)dy} \qquad [6\text{-}5]$$

where b = *ln(1 000 000)*, e is the natural number 2.7182..., y is a dummy variable of integration representing the logarithm of soil suction and Θ^q is a correction factor, where Θ is the normalised volumetric water content or relative degree of saturation as:

$$\Theta=\frac{\theta-\theta_r}{\theta_s-\theta_r} \qquad [6\text{-}6]$$

Fredlund *et al.* (1994) indicate that Equation 6-5 can be solved by numerical integration. The relative hydraulic conductivity as a function of soil suction can be expressed as:

$$K_r(\psi)=\frac{\sum_{i=j}^{N}\frac{\theta(e^{\bar{y}_i})-\theta(\psi)}{e^{\bar{y}_i}}\theta'(e^{\bar{y}_i})}{\sum_{i=1}^{N}\frac{\theta(e^{\bar{y}_i})-\theta_s}{e^{\bar{y}_i}}\theta'(e^{\bar{y}_i})} \qquad [6\text{-}7]$$

where N is the number of intervals and $\bar{y}_i$ is the midpoint of the ith interval.

A computer programme, UNSAT.K was developed in Delphi language to conduct the numerical integration required by the Fredlund *et al.* (1994) model. Soil-water retention data is fitted to the Fredlund and Xing (1994) function and the parameters a, n, m and Cr, required to describe the soil-water characteristic curve, are determined. These values are entered into the computer program. The computer program calculates the volumetric water content and unsaturated hydraulic conductivity at specified soil suction values, applying Equations 6-5 and 6-7.

It has already been shown that the soil-water characteristic curves for five soil types can be accurately described by the Van Genucten (1980) and Fredlund and Xing (1994) functions. These data-sets were further analysed to determine the unsaturated hydraulic conductivity in term of the Van Genucten (1980) and Fredlund *et al.* models. The calculated values were compared to experimentally determined unsaturated hydraulic conductivity values. The results are shown in **Figures 6.12** to **6.15**.

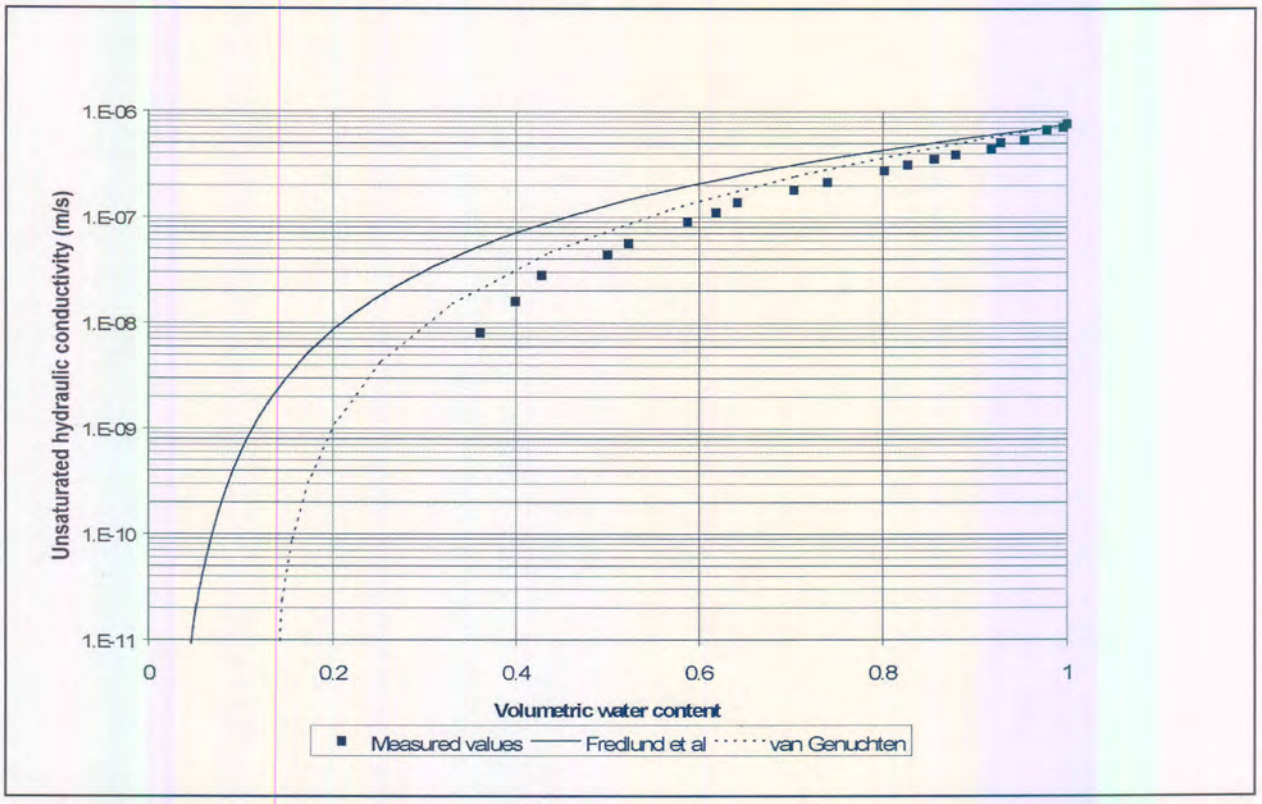

Figure 6.12: Correlation between measured and predicted unsaturated hydraulic conductivity based on soil-water characteristic curves: Sand

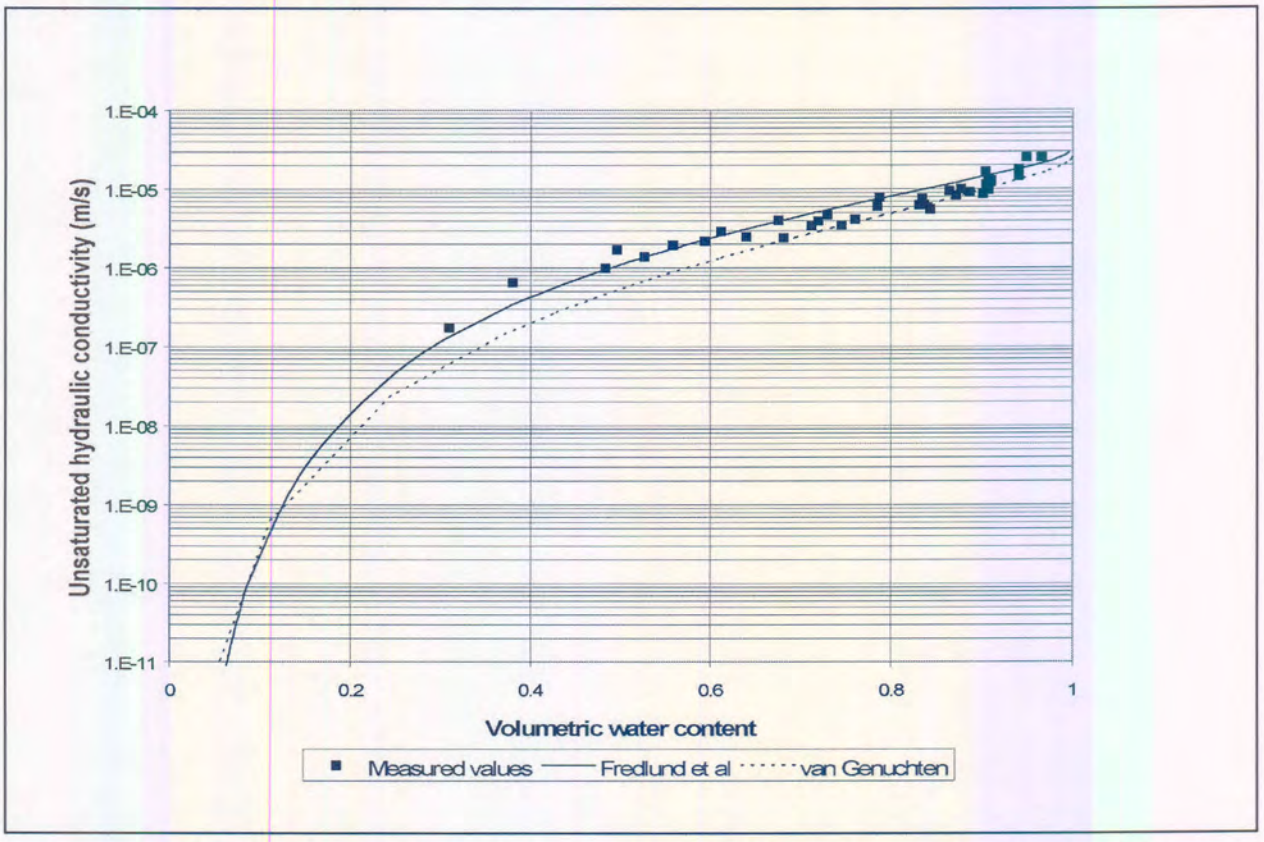

Figure 6.13: Correlation between measured and predicted unsaturated hydraulic conductivity based on soil-water characteristic curves: Fine sand

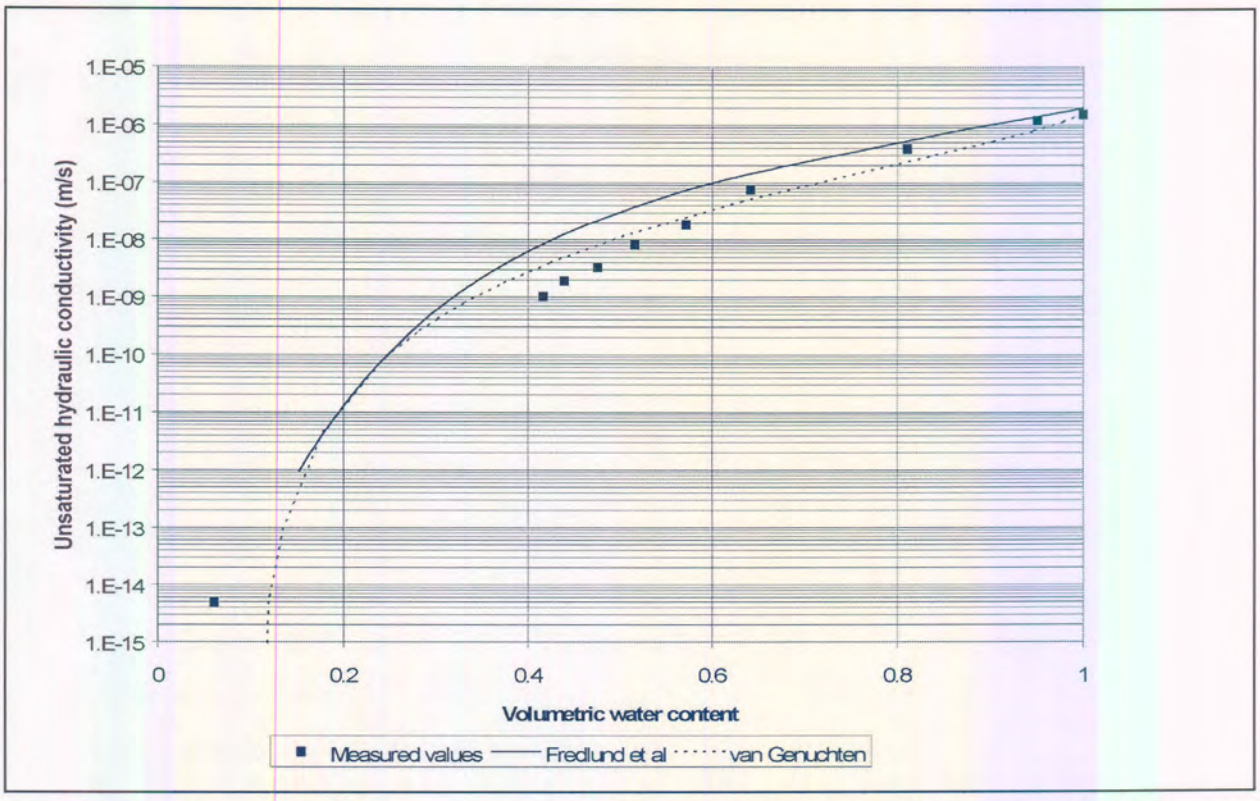

Figure 6.14: Correlation between measured and predicted unsaturated hydraulic conductivity based on soil-water characteristic curves: Sandy silt-clay

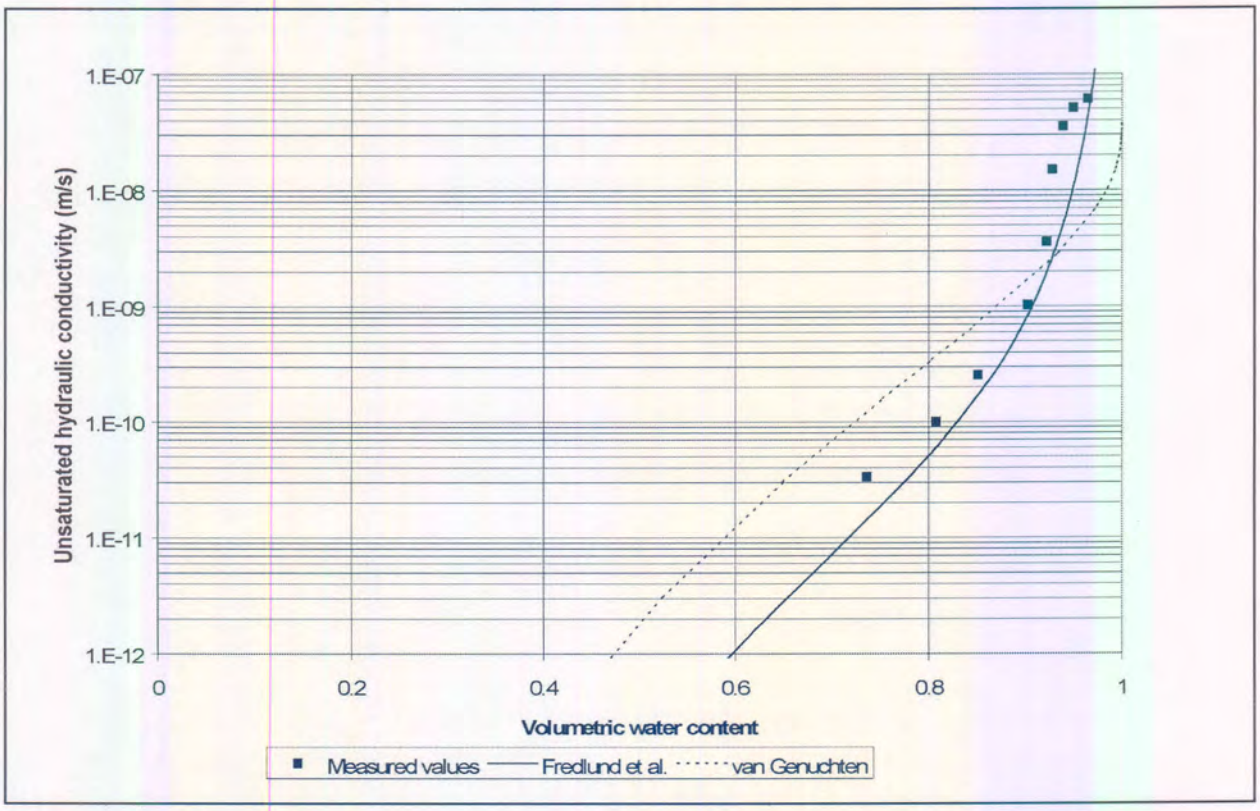

Figure 6.15: Correlation between measured and predicted unsaturated hydraulic conductivity based on soil-water characteristic curves: Clay

Sand

From the above data it can be concluded that the Van Genucten (1980) model can accurately predict the unsaturated hydraulic conductivity. In contrast, the Fredlund *et al.* (1994) model slightly overestimate unsaturated hydraulic conductivity, but the predictions are adequate for most field applications. The unsaturated hydraulic conductivity curve of sand is characterised by a sharp inclination point, indicating that water drains from the large pores and that the retained water is strongly adsorbed to the soil grains. Of interest is the uncharacteristically low saturated hydraulic conductivity measured for the specific sand used in the analyses, which is lower than both the saturated hydraulic conductivity of fine sand and sandy silt-clay. This indicates that saturated hydraulic conductivity is not a function of particle-size distribution only.

Fine sand

Both the Van Genuchten (1980) and Fredlund *et al.* (1994) models accurately predict the unsaturated hydraulic conductivity, with the latter achieving a slightly better correlation. The curve is characterised by a more gradual slope than is the case with sand, indicating that water is retained in the smaller pores and is gradually removed by higher suctions up to about 40 per cent water content, where after the unsaturated hydraulic conductivity decreases rapidly in accordance with the decrease in water content.

Sandy silt-clay

As with the fine sand, both the Van Genuchten (1980) and Fredlund *et al.* (1994) functions fairly accurately describe the unsaturated hydraulic conductivity of sandy silt-clay, although not as accurately as with the fine sand. Deviations between 0 per cent and 40 per cent of water content occur. However, predicted unsaturated hydraulic conductivity is adequate for most field applications.

Clay

The unsaturated hydraulic conductivity curve differs considerably from that of the sand, fine sand and sandy silt-clay. Because of the large surface area of clay minerals, water is strongly adsorbed to the clay minerals and does not drain easily. It can be seen that the Fredlund *et al.* (1994) function gives a much more accurate prediction of unsaturated hydraulic conductivity than the Van Genuchten (1980) function. However, the Fredlund *et al.* (1994) function indicates that the unsaturated hydraulic conductivity values at near-saturated conditions are higher than saturated hydraulic conductivity and that is obviously not possible. With the exception of this inherent error, the Fredlund *et al.* (1994) function accurately predicts the unsaturated hydraulic conductivity of clay.

The correlation coefficients for the various soil types are indicated in **Table 6.15**. It appears that the Van Genuchten (1980) function better represents sandy soils, while the Fredlund *et al.* (1994) function better represents clayey soils. These findings corroborate the findings of Leong & Rehardjo (1997b) that the Fredlund *et al* (1994) function does not predict unsaturated hydraulic conductivity of sandy material as well as the Van Genuchten (1980) model.

Table 6.15: Correlation between estimated and experimentally derived unsaturated hydraulic conductivities (at selected water contents)

Soil type	Coefficient of correlation	
	Van Genuchten	Fredlund *et al.*
Sand	0.9855	0.9657
Fine sand	0.9515	0.9067
Sandy silt-clay	0.9998	1.0000
Clay	0.6535	0.9990

Application of unsaturated hydraulic conductivity models to the field experimental sites

Predictions of unsaturated hydraulic conductivity were made from soil-water characteristic curves based on the models developed by Van Genuchten (1980) and Fredlund *et al.* (1994), as was discussed in the preceding section. The computer program UNSAT.K was applied to determine unsaturated hydraulic conductivity as a function of volumetric water content, based on the permeability and soil-water retention test results for Experiments 1 & 2, 3 & 4 and 5.

After the water retention data had been obtained for residual soils at the respective experimental sites, the data were fitted to soil-water characteristic functions as developed by Van Genuchten (1980) and Fredlund and Xing (1994). The parameters necessary to describe the soil-water characteristic curves were determined. The methodology to determine the fitting parameters from soil-water retention and permeability data was identical to that described in Section 6.3.

With the fitting parameters, saturated hydraulic conductivity and porosity values known, the unsaturated hydraulic conductivity, as a function of water content could be determined. The data were applied to the restricted Van Genuchten (1980) and the Fredlund *et al* (1994) models and these have been discussed in the preceding section.

The results, indicating unsaturated hydraulic conductivity as a function of volumetric water content, are shown in **Table 6.16**.

Table 6.16: Unsaturated hydraulic conductivity at various soil suction values

Soil suction (kPa)	Experiments 1 and 2		Experiments 3 and 4		Experiment 5	
	K (VG)	K (F)	K (VG)	K (F)	K(VG)	K (F)
1.00	1.1×10^{-10}	9.7×10^{-10}	1.4×10^{-8}	5.0×10^{-7}	7.0×10^{-7}	1.2×10^{-6}
5.00	2.6×10^{-12}	1.9×10^{-11}	1.4×10^{-10}	5.4×10^{-10}	2.2×10^{-7}	3.7×10^{-7}
10.00	3.6×10^{-13}	3.4×10^{-12}	1.4×10^{-11}	1.0×10^{-10}	8.4×10^{-8}	1.7×10^{-7}
20.00	4.6×10^{-14}	6.6×10^{-13}	1.4×10^{-12}	2.3×10^{-11}	2.3×10^{-8}	6.1×10^{-8}
50.00	3.0×10^{-15}	8.2×10^{-14}	6.7×10^{-14}	3.4×10^{-12}	2.6×10^{-9}	1.0×10^{-8}
100.0	3.7×10^{-16}	1.8×10^{-14}	6.5×10^{-15}	7.8×10^{-13}	4.0×10^{-10}	1.8×10^{-9}
1000	3.5×10^{-19}	1.2×10^{-16}	2.9×10^{-18}	5.9×10^{-15}	5.9×10^{-13}	2.6×10^{-12}

VG = Van Genuchten (1980)
F = Fredlund *et al* (1994)

Unfortunately, the predicted unsaturated hydraulic conductivities could not be compared to *in situ* values measured at the experimental sites. Because of the simple way in which unsaturated hydraulic conductivity is derived by means of internal drainage tests, accurate estimations of unsaturated hydraulic conductivity may not be attainable. Notwithstanding, unsaturated hydraulic conductivity values for Experiment 4 compare well with that predicted by the Van Genuchten (1980) model. However, discrepancies do occur at higher water contents, which occur due to inherent errors of the Lax-θ method used to determine the unsaturated hydraulic conductivity.

In general, the shape of the unsaturated hydraulic conductivity curve as predicted by the Van Genuchten (1980) and Fredlund *et al.* (1994) functions compare well with each other, even though the predicted unsaturated hydraulic conductivity as derived from the Van Genuchten (1980) model is consistently slightly lower, compared to predicted values derived from the Fredlund *et al.* (1994) function. The similar unsaturated hydraulic conductivity values might indicate that both the Van Genuchten (1980) and Fredlund *et al* (1994) functions were successful in accurately predicting the unsaturated hydraulic conductivity as a function of soil water content.